Technical Report No. 55

WATER FOR UTILITIES: CLIMATE CHANGE IMPACTS ON WATER QUALITY AND WATER AVAILABILITY FOR UTILITIES IN EUROPE

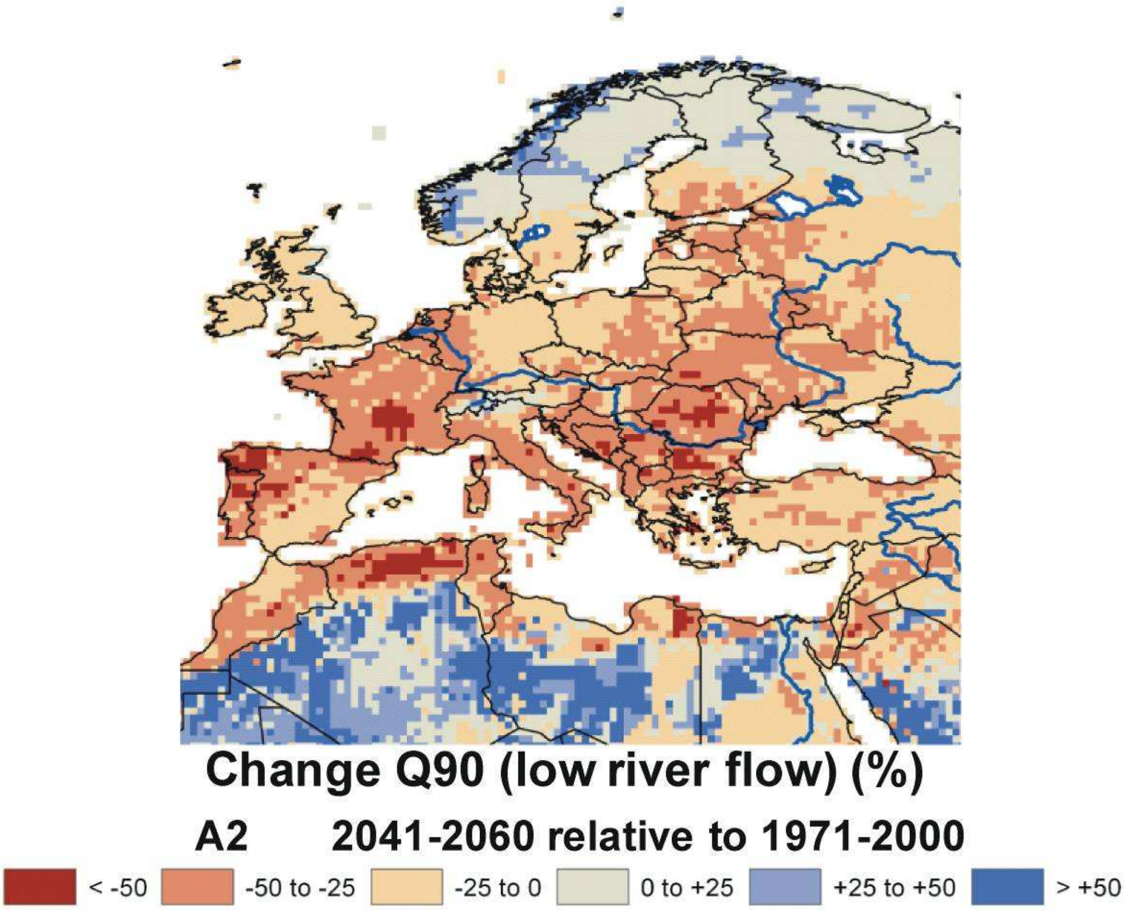

Author names: J.J.G. Zwolsman, M. van Vliet, M. Bonte, N. Gorski, M. Flörke, S. Eisner & F. Ludwig

Date: September 15th, 2011

WATCH is an Integrated Project Funded by the European Commission under the Sixth Framework Programme, Global Change and Ecosystems Thematic Priority Area (contract number: 036946).
The WACH project started 01/02/2007 and will continue for 4 years.

Title:	Water for utilities: Climate change impacts on water quality and water availability for utilities in Europe
Authors:	J.J.G. Zwolsman, M. van Vliet, M. Bonte, N. Gorski, M. Flörke, S. Eisner & F. Ludwig
Organisations:	KWR Watercycle Research Institute, Wageningen University & Research Centre and University of Kassel
Submission date:	September 15th, 2011
Function:	This report is the output from Work Block 6; task 6.3.4
Deliverable	WATCH deliverable 6.3.4

Contents

1 Introduction

Observational records and climate projections provide abundant evidence that freshwater resources have the potential to be strongly impacted by climate change, with wide-ranging consequences for human societies and ecosystems (see e.g. EEA, 2007; EEA, 2008a; IPCC, 2008). Various aspects of the hydrological cycle are affected by climate change, e.g. precipitation, evaporation, sea level rise, snowmelt, river discharge, groundwater recharge, and so on. The amount of snow storage is critical for water supply and environmental needs in catchments fed by snowmelt, but so is the timing of snowmelt runoff into rivers and streams. Along with reductions in the amount of the snowpack and accelerated snowmelt, scientists project greater storm intensity, resulting in more direct runoff and flooding. Changes in watershed vegetation and soil moisture conditions will likewise change runoff and recharge patterns. As stream flows and velocities change, erosion patterns will also change, altering channel shapes and depths, possibly increasing sedimentation behind dams, and affecting habitat and water quality. With potential increases in the frequency and intensity of wildfires due to climate change, there is a potential for more floods following fire, which increase sediment loads and water quality impacts.

Due to its tremendous impact on the hydrological cycle, climate change is highly relevant to the water sector (IWA, 2009; EEA, 2011). Warming temperatures, combined with changes in rainfall and runoff patterns will exacerbate the frequency and intensity of droughts and floods. Regions that rely heavily upon surface water (rivers, streams, and lakes) could be particularly affected as runoff becomes more variable, and more demand is placed on groundwater to overcome periods of droughts. For example, model calculations indicate that the hydrology of the Rhine River will change towards higher winter discharges and lower summer discharges ((Middelkoop et al. 2001; Lenderink et al. 2007; Hurkmans et al., 2010). These changes are attributed to intensified snowmelt and increased precipitation from winter to spring, and a reduced contribution from snowmelt combined with an increase of evapotranspiration during the summer. Consequently, an increased risk of floods and drought is foreseen for the Rhine.

In addition, climate change has strong implications for water quality as well, which are just becoming recognized (EEA, 2007; IPCC, 2008). These changes in water quality pose challenges to water treatment processes for drinking water and industrial purposes (Delpla et al., 2009; IWA, 2009). Climate change will also affect water demand. Warmer temperatures will increase evapotranspiration rates and extend growing seasons, thereby increasing the amount of water that is needed for crop irrigation, urban landscaping and environmental water needs (ecological flows). Domestic water use typically shows peak demands during hot spells. There may not be enough water available to fulfill the needs of all water consumers during droughts, leading to increasing competition between water users, forcing regulation by the local authorities or state government.

This report provides an assessment of the consequences of changing water availability for production of drinking water, the manufacturing industry and power production in Europe, due to climate change and socio-economic developments. The report is based upon projections of demographic and socio-economic trends and climate change impacts, according to the SRES A2 and B1 scenario’s also used by IPCC. Chapter 2 deals with water quality impacts of climate change in a European context, focusing solely on chloride and water temperature. Chapter 3 deals with water demand of domestic and industrial water use (manufacturing and power production), water availability and water stress on a European scale, as projected for the time horizons 2050 and 2100.

2 Climate change and water quality

2.1 Introduction

The impact of climate change on the hydrological cycle has been studied widely, with a clear focus on water quantity. Research on the water quality impacts of climate change is very limited, but growing. Beside human influences, it is obvious that water quality depends on climate-related variables such as water temperature and river flows. One of the first review papers on the topic was written by Murdoch et al. (2000). In their comprehensive review, changes in water quality were related to hydrological factors (e.g. limited dilution of point sources during low river flows, or increased runoff from agricultural land during rainstorms), terrestrial factors (e.g. changes in vegetation and soil structure) and resource-use factors (e.g. increased water use, increased demand for cooling capacity). More recently, reviews on the topic have been written by EEA (2007) and Delpla et al. (2009), and case studies were published by Zwolsman & van Bokhoven (2007) and Van Vliet & Zwolsman (2008). In general, it is concluded that climate change has a negative impact on water quality, especially during summer droughts, due to high water temperatures and low river flows. On the other hand, it is also reported that the chemical loading of surface waters from non-point sources (e.g. soil leaching), which depends on the amount and intensity of rainfall in the catchment area, may decrease during droughts (e.g. Krysanova et al., 2005).

Changes in the timing of river flows and warming atmospheric temperatures may affect water quality and water uses in many different ways. At one extreme, flood peaks may cause more erosion, resulting in turbidity and concentrated pulses of pollutants. This will challenge water treatment plant operations to produce safe drinking water. Flooding can also threaten the integrity of water works infrastructure. At the other extreme, lower summer and fall flows may result in greater concentration of contaminants due to limited of dilution of industrial and communal waste water (e.g. Van Vliet & Zwolsman, 2008). These changes in stream flow timing, especially the increase in low flow periods, may require new approaches to discharge permitting of point source pollution. Warmer water will distress many fish species and could require additional cold water reservoir releases. Higher water temperatures can also accelerate some biological and chemical processes, increasing growth of algae and microorganisms, the depletion of dissolved oxygen, and various impacts to water treatment processes. An increase in the frequency and intensity of wildfires will also affect watersheds, vegetation, runoff and water quality (EEA, 2007).

In this chapter, water quality impacts of climate change are discussed in a European context, focusing on chloride and water temperature.

2.2 Chloride - runfoff relations for selected river systems

The influence of river flow on chloride concentration has been studied for three major European rivers: the Elbe, the Rhine and the Danube. Originally, the plan was to study these relations in the pilot areas of the WATCH project, but it turned out to be very difficult to obtain water quality information for most of the study basins. Therefore, we selected three major European river systems for our study, including two small branches of the Elbe (Sazava) and the Danube (Nitra). An overview of the available data and the basic statistics for chloride concentration and river discharge is shown in Table 2.1. Based on the data, it can be concluded that the pollution status of the rivers with respect to chloride varies form unpolluted (Savaza, Nitra at station Klacno), slightly polluted (Danube, stations Bratislava and Bazias), moderately polluted (Danube, station Chichiu; Elbe, station Decin) to heavily polluted (Rhine, station Lobith; Nitra, station Nitrianska). The unpolluted streams (Upper Nitra, Savaza) are headwaters which show chloride concentrations on the order of 10 mg/l, typical of pristine conditions. The slightly polluted rivers show chloride concentrations on the order of 20 mg/l; the moderately polluted rivers around 35 mg/l, and the strongly polluted rivers around 100 mg/l.

Table 2.1: Overview of available data and basic statistics (minimum, maximum, median) of the dataset for chloride and river discharge

River	Location	Period	N	Q min (m3/s)	Q max (m3/s)	Q med (m3/s)	Cl min (mg/l)	Cl max (mg/l)	Cl med (mg/l)
Rhine	Lobith	1990-2008	510	793	11790	1911	29	322	107
Elbe	Decin	1993-2000	138	104	1370	221	14	53	33
Savaza	Savazou	1977-2006	343	0,08	8,4	0,69	4	43	11
Nitra	Klacno	1975-2006	367	0,03	1,44	0,16	1,1	43	9
Nitra	Nitrianska	1975-2006	364	2,8	58	10	14	568	106
Danube	Bratislava	1996-2006	248	888	7678	1867	9	40	17
Danube	Bazias	1997-2006	159	1650	12669	4900	12	36	21
Danube	Chichiu	1997-2006	142	1925	15300	6029	19	85	34

For non-reactive substances such as chloride, the concentration depends on human input, background concentration and the river discharge (Van der Weijden and Middelburg, 1989), according to:

$$C = \frac{a}{Q} + b\,,$$

In which C = the concentration (mg/l); Q = discharge (m^3/s); a = human input (g/s) and b = background concentration (mg/l).

We fitted the available dataset (Table 2.1) to this equation; the results are shown in Table 2.2 and Figure 2.1.

Table 2.2. Overview of chloride – runoff relationships in the selected river systems

river	location	period	a (g/s)	b (mg/l)	R^2
Rhine	Lobith	1990-2008	140681	40	0,579
Elbe	Decin	1993-2000	2528	22	0,529
Savaza	Savazou	1977-2006	0,44	12	0,010
Nitra	Klacno	1975-2006	-0,06	11	0,004
Nitra	Nitrianska	1975-2006	847	31	0,441
Danube	Bratislava	1996-2006	11171	12	0,196
Danube	Bazias	1997-2006	11503	19	0,105
Danube	Chichiu*	1997-2006	43004	26	0,196

* five outliers were deleted from the dataset

From Table 2.2 it can be observed that significant relations between chloride concentration and river flow may exist for moderately to strongly polluted river systems, such as the Rhine, the Elbe and the Nitra river at Nitrianska (see also Figure 2.1). For slightly polluted and unpolluted river systems, the relation cannot be established. This can easily be understood as the pollution load for chloride is mainly related to industrial and municipal point sources which will become less diluted during low river flows. In slightly polluted or pristine conditions, the chloride concentration will lie close to the natural background which is relatively insensitive to changes in river flow.

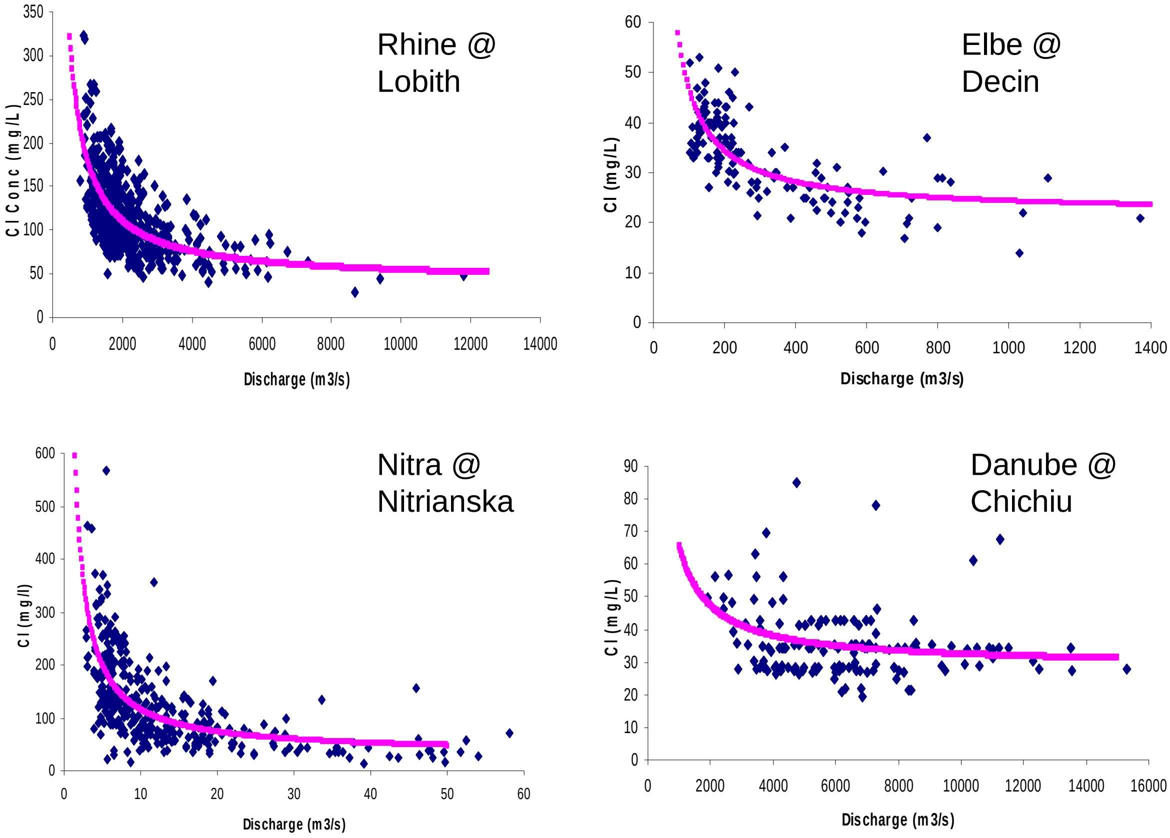

Figure 2.1: Relationship between chloride concentration and river discharge for some moderately to strongly polluted European rivers (see also Table 2.2).

The results show that climate change may have a serious impact on the chloride concentration of river systems which are already moderately to strongly polluted, because of the increase of low flow periods (in frequency and intensity) with minimal dilution. This may have consequences for sectors as drinking water supply, industrial water supply and agriculture if water quality standards are exceeded (e.g. the drinking water standard of 250 mg/l).

2.3 Salinization of Lake IJsselmeer: consequences for water supply

2.3.1 Introduction

Lake IJsselmeer and Lake Markermeer form the largest artificial freshwater system in north-western Europe and are fed primarily by the Rhine River. Both lakes are an important source of freshwater for drinking water production, agriculture and industry in the Netherlands. After World War II, increasing salinisation occurred due to emissions mainly from potash and brown coal mining activities in the catchment area, causing the water quality of the Rhine River and Lake IJsselmeer to deteriorate with chloride concentrations in excess of 400 mg/l. Growing concern regarding the water quality of the Rhine River led to a series of treaties and plans which aimed to reduce salt emissions and improve the quality of the river water. As a result, the average annual chloride concentration gradually declined to values around 100 mg/l nowadays. However, peak values close to 200 mg/l are still observed in the Rhine at the Dutch-German border during periods of low river flow, e.g. summer-autumn 2003 (Zwolsman & Van Bokhoven, 2007). Hydrological modelling has shown that the frequency and duration of such low flow periods are likely to increase as a result of climate change (Middelkoop et al., 2001; Shabalova et al., 2003). This suggests that the impacts of climate change are of great importance to future water supply in the Netherlands. Chloride is especially relevant for drinking water production as it is a compound that is not removed by conventional water treatment techniques.

Recently, Bonte & Zwolsman (2010) published a modelling study to investigate the impacts of climate change and associated hydrological shifts on the chloride concentration and salinisation processes in the Lake IJsselmeer region. The model was used to elucidate the salinisation processes occurring under present hydrological conditions and to assess future salinisation under two climate forcing scenarios. A summary of the results is presented in this paragraph. Details on the construction, calibration and validation of the model can be found in the original paper (Bonte & Zwolsman, 2010).

2.3.2 Study Site

Lakes IJsselmeer and Markermeer are part of a larger system of connected freshwater lakes referred to as the IJsselmeer region, situated in the northern part of The Netherlands (see Figure 2.2). Table 2.3 shows the main physiographical characteristics of the two lakes.

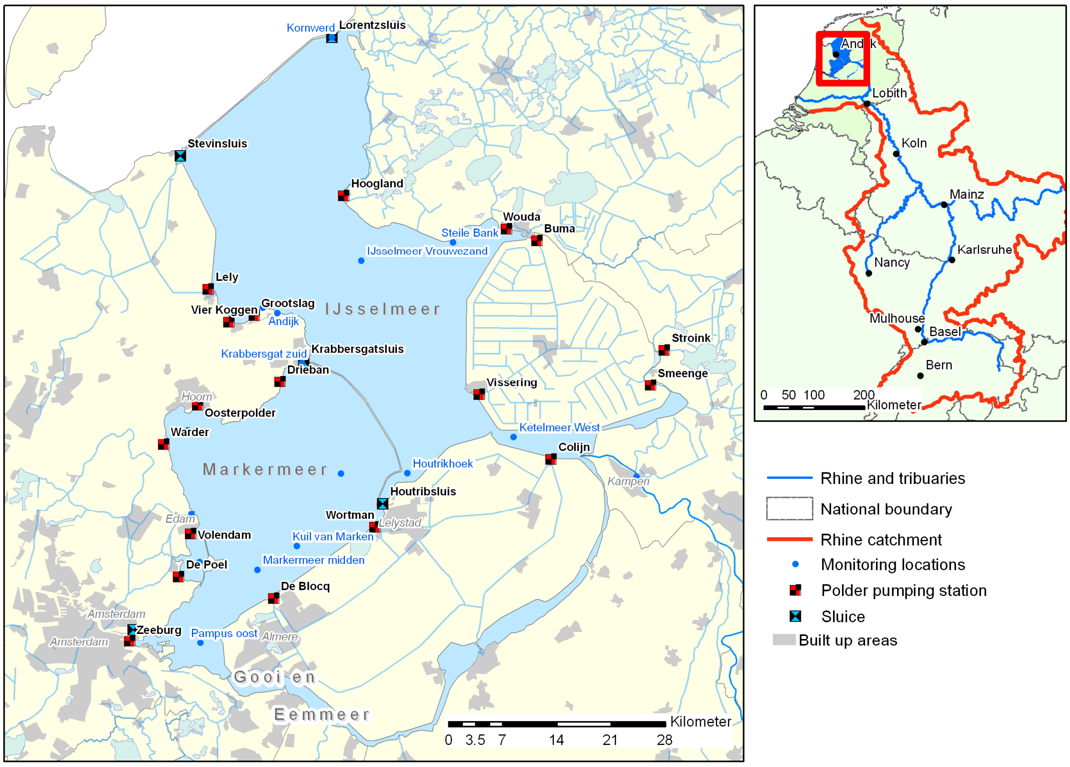

Figure 2.2. Map of Lake IJsselmeer and Lake Markermeer, situated in the northern part of the Netherlands

Table 2.3. Physiographical characteristics of lakes IJsselmeer and Markermeer

	IJsselmeer	Markermeer
Surface area (km^2)	1080	700
Average depth (m)	4.7	3.9
Residence time (month)	3-4	15-18

Lake IJsselmeer was created in 1932 by the construction of a 30 km long tidal closure dam, separating the Wadden Sea from the former estuary (Figure 2.2). Initially, Lake IJsselmeer was a large brackish lake that gradually freshened up as water from the river IJssel (the northern branch of the Rhine river in the Netherlands) continuously flushed the water system. In 1976, lakes IJsselmeer and Markermeer were physically separated by the completion of a dam. Two sluices in the dam control water transfer between the two lakes. Today, lake IJsselmeer receives most of its water from the River IJssel (70% on average), which is essentially Rhine water. The other sources of water to the lake include rainfall, exchange with Lake Markermeer and a number of polders that drain directly to the lake. The main inputs of water to Lake Markermeer are exchange with Lake IJsselmeer, rainfall and polder drainage.

2.3.3 Chloride sources to the lakes

To gain an understanding of the salinisation processes occurring in Lake IJsselmeer and Lake Markermeer, the model was used to determine the contribution of the different water sources to the chloride concentration in Lake IJsselmeer at the water supply intake station (Andijk) and in central Lake Markermeer. This was done by first running the calibrated model only including water and chloride inputs from the IJssel River, followed by a number of model runs where one source of water and chloride is consecutively added to the model. The results of this analysis are presented in Figure 2.3.

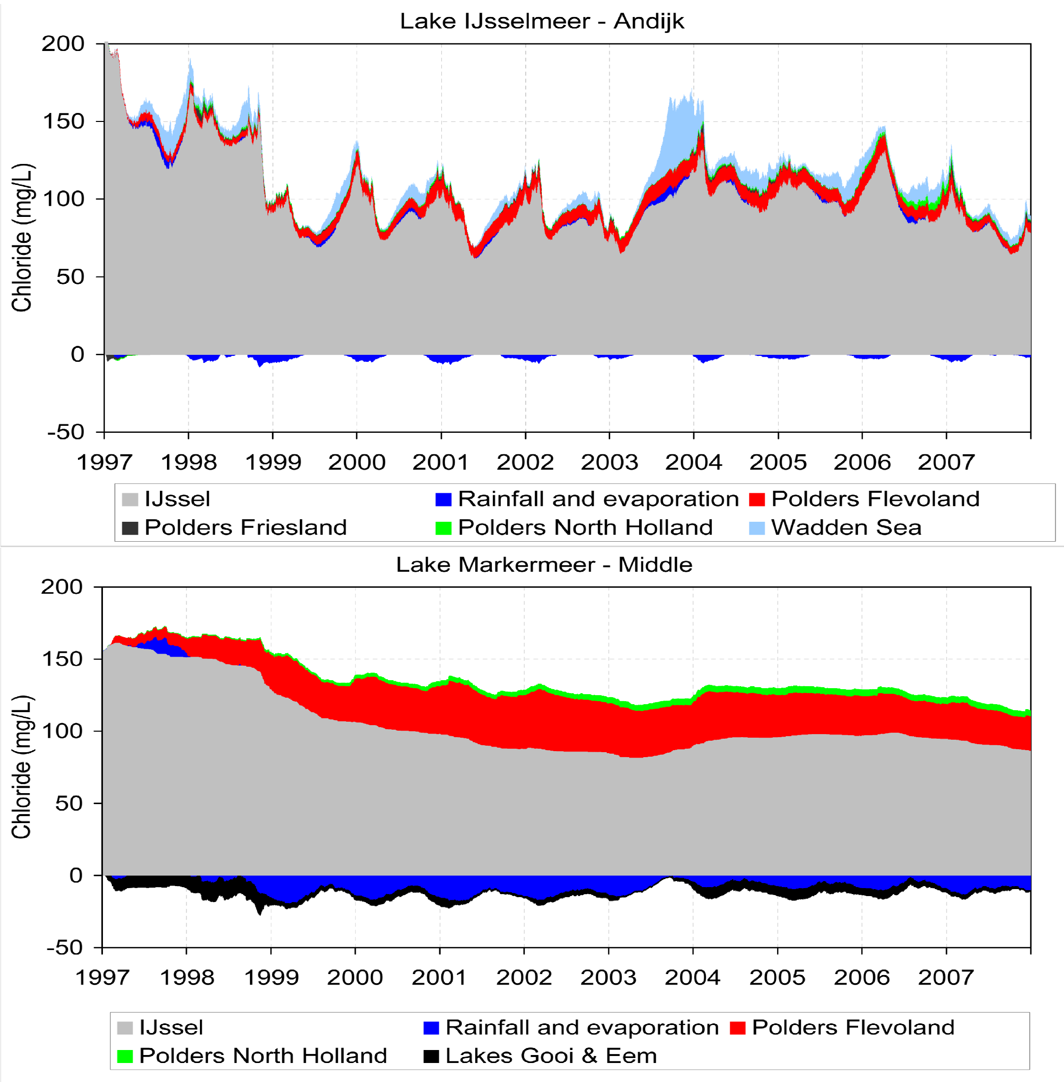

Figure 2.3. Sources of chloride to Lake IJsselmeer and Lake Markermeer in the period 1997-2007.

The simulation clearly shows that the IJssel River (i.e., Rhine water) is the main source of chloride to both lakes. In Lake Markermeer, discharges from the surrounding polder areas increase the chloride concentration while the net rainfall (rainfall minus evaporation) and inflow from lake Gooi & Eem have a decreasing effect (dilution) on the chloride concentration. This clearly reflects the differences in chloride concentrations of the individual water sources to the lake.

In Lake IJsselmeer, the main sources of chloride besides the IJssel River are sea water intrusion across the tidal closure dam, due to seepage and direct intrusion through the shipping locks, and drainage from the Flevoland polder. In the relatively dry summer and fall of 2003, sea water intrusion across the tidal closure dam was simulated to have a relatively large contribution of around 50 mg/l to the total chloride concentration at station Andijk. This input of chloride from the Wadden Sea, together with the high chloride concentrations in the Rhine at that time, caused the chloride concentration at Andijk to exceed the drinking water standard of 150 mg/l in the fall of 2003. The simulation also shows that in all other simulated years, the contribution of sea water intrusion to the chloride concentration at Andijk is far less. This difference is probably due to higher discharge from Lake IJsselmeer to the Wadden Sea during average or wet years, which flushes out the seawater introduced through the tidal closure dam.

2.3.4 Impact of climate change on the salinisation process

To assess the impact of climate change on the chloride concentration of the lakes, all relevant input data (e.g. river flow, polder drainage, sea level) for the period 1997-2007 was transformed to the reference year 2050 using two climate change scenarios developed by the Royal Dutch Meteorological Institute (KNMI). These two scenarios, named G (moderate) and W+ (warm), span the total range of the four climate change scenarios developed by KNMI (Van den Hurk et al., 2006). This means that the results of our simulations provide a band width for the expected impact of climate change on chloride concentration in Lake IJsselmeer and Markermeer. The results of the climate change simulations are compared to the reference scenario based on present climate and hydrology for 2007-2008 (Figure 2.4).

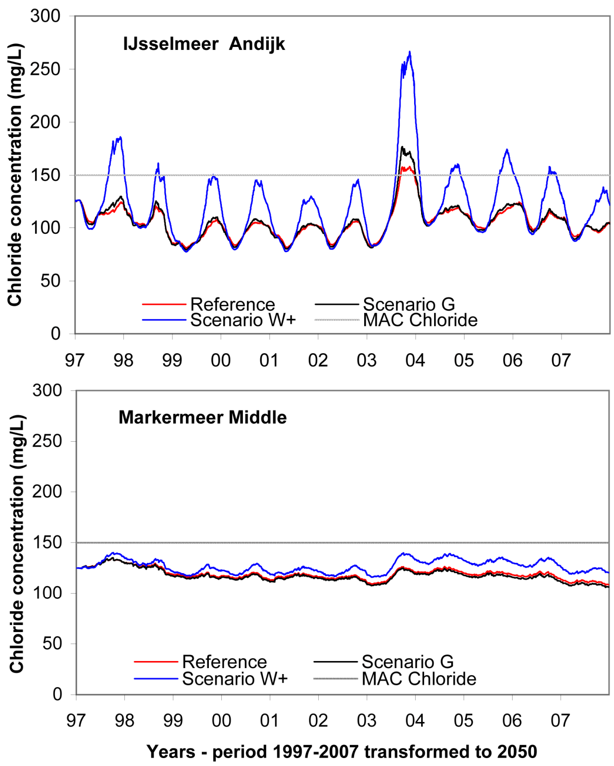

Figure 2.4. Projected chloride concentration of Lake IJsselmeer and Lake Markermeer in 2050.

The results clearly show that the largest effects occur in Lake IJsselmeer in climate scenario W+. The chloride concentration at raw water intake station Andijk under scenario W+ shows an increase of 30 to 50 mg/l during average summers (compared to the reference situation), increasing to over 100 mg/l under extremely dry conditions (year 2003, transformed to 2050). The daily probability of exceeding the chloride standard for drinking water in Lake IJsselmeer (Andijk) increases from 2.5% for the reference scenario to 14.3% for climate change scenario W+. The maximum duration of standard exceedance increases from 103 days in the reference scenario to 178 days in the W+ scenario (both in the year 2003, transformed to 2050). For scenario G, concentrations in Lake IJsselmeer increase only slightly compared to the reference situation. The effects of climate change on Lake Markermeer are relatively small, due to the large residence time of this lake, levelling out peak concentrations in summer and fall.

Similar to the chloride source analyses presented in Figure 2.3 for the present situation, Figure 2.5 presents the stacked changes in chloride concentration between the reference period and the year 2050 due to: i) changing hydrology of the Rhine; ii) changing rainfall and precipitation patterns; iii) changing intrusion from the Wadden Sea; and iv) changing chloride input from polders directly draining to Lake IJsselmeer (emissions of chloride were assumed to be constant between the reference period and the year 2050).

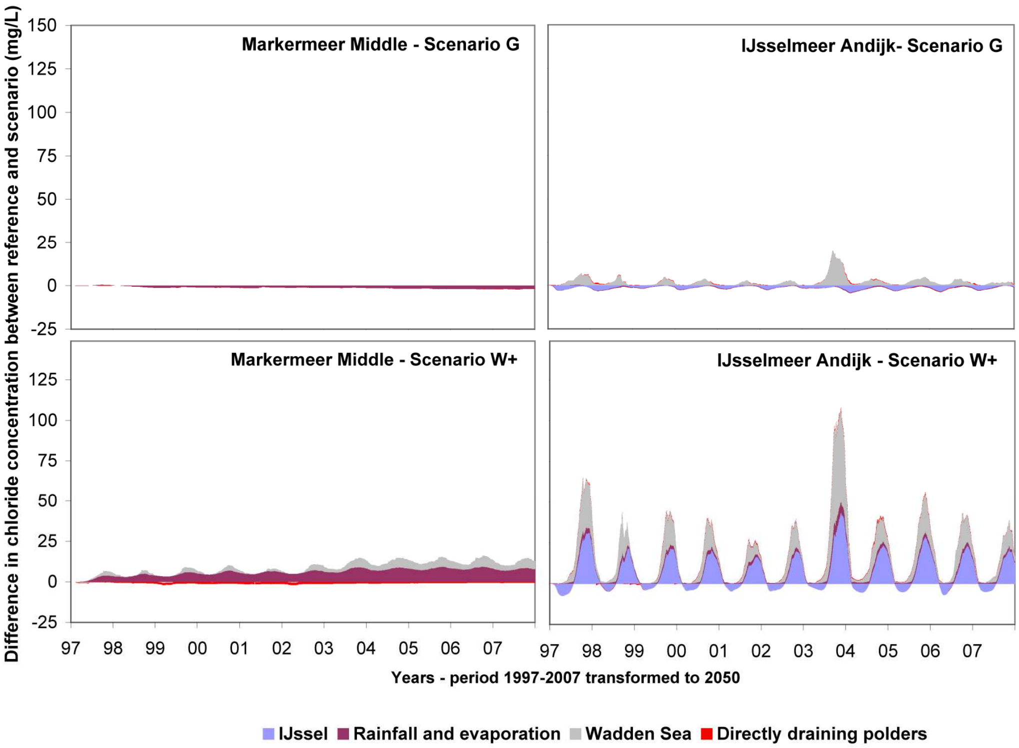

Figure 2.5: Origin of surplus chloride in Lake IJsselmeer and Lake Markermeer in 2050

From Figure 2.5 it can be seen that a large fraction of the chloride change in Lake IJsselmeer is due to the increased intrusion of salt water from the Wadden Sea and the changing hydrology of the Rhine. Rising sea levels increase the head difference between the Wadden Sea and Lake IJsselmeer, causing more seawater intrusion via seepage through the closure dam and direct intrusion through the shipping locks. The modelling suggests that the reduction of through flow in Lake IJsselmeer during droughts leads to less efficient flushing of this salt load, allowing further dispersion of the salt load into the lake, with notable influence at freshwater abstraction location Andijk. Moreover, reduced summer flows also cause less dilution of the chloride load of the Rhine River, resulting in a higher chloride concentration in the river water (see Figure 2.1) which propagates into the IJssel branch and Lake IJsselmeer.

The results show that in order to keep Lake IJsselmeer sufficiently fresh for year round drinking water production (limit 150 mg/l chloride), a further reduction of salt emissions to the Rhine or a reduction of seawater seepage from the Wadden Sea (through technical engineering measures) is required. The modelling shows that Lake Markermeer is actually a more suitable source for drinking water production than Lake IJsselmeer as it is less susceptible to climate change induced salinisation. The possibility to control water transfers from Lake IJsselmeer to Lake Markermeer also makes it a better raw water source from the perspective of other pollutants present in river water, especially during chemical spills and other calamities on the Rhine River. As a result, Lake Markermeer can be considered a water conservation reservoir for the Lake IJsselmeer region.

2.4 Modelling river water temperature

The sensitivity of river water temperature to climate change was studied on a global scale by *van Vliet et al.* [2011]. The sections below summarize the methodology and the major results of this published study.

2.4.1 Introduction

Water temperature is an important physical property of rivers, having a direct impact on water quality (e.g. dissolved oxygen concentration) and on growth rate and distribution of freshwater organisms. Additionally, river temperature is of economic importance in water requirements for industry, electricity and drinking water production, and recreation [*Webb et al.*, 2008]. Several studies found a gradual increase in river temperatures during the last century in relation to an increase in air temperatures [*e.g. Liu et al.*, 2005; Webb & Nobilis, 2007]. In addition, rising water temperatures have also been related to changes in river flow. For example, for the Danube an increase in water temperature was observed as a consequence of lower summer flow, resulting from earlier onset of the snowmelt period and decreased summer precipitation [*Pekarova et al.*, 2008]. Water temperature trends in major rivers over the past century are thus a complex function of both climate and hydrological changes [*Webb and Nobilis*, 2007]. In addition, anthropogenic influences, like thermal effluents from power stations [*Webb and Nobilis*, 2007], flow regulation and construction of reservoirs [*Lowney*, 2000; *Webb and Walling*, 1993], and land use changes, e.g. urbanization [*Nelson and Palmer*, 2007], also affect water temperature. These anthropogenic influences vary considerably between catchments and river basins [*Caissie*, 2006].

Air temperature is commonly used as a predictor variable in water temperature regression models, because it is a major component in calculating net changes of heat flux at the water surface [*Webb et al.*, 2003; *Webb et al.*, 2008]. As a result, there is a strong correlation between air and water temperatures. Linear water temperature regression models have been widely applied using weekly and monthly mean values of water temperature [*e.g. Webb and Walling*, 1993; *Webb and Nobilis*, 1997]. Although several studies have demonstrated that water temperature is inversely related to river discharge, reflecting a reduced thermal capacity under decreasing flow volumes [*e.g. Webb*, 1996; *Webb et al.*, 2003], only a few addressed the influence of river flow on the water - air temperature relationship or included river discharge as an additional variable into water temperature regression models [*Ozaki et al.*, 2003; *Rivers-Moore and Jewitt*, 2007; *Webb et al.*, 2003]. A multiple linear regression analysis of *Webb et al.* [2003] showed that an inverse relation between water temperature and discharge exists for all catchments and timescales, with greater impact at shorter timescales and in larger catchments of the Exe basin (UK). Limited knowledge, however, exists with regard to the influence of discharge on water temperatures for large river basins.

Against this background, we have developed a nonlinear water temperature regression model relating river water temperature to both air temperature and river flow. The model was used to quantify the sensitivity of river temperatures to both atmospheric warming and changes in river flow. In this section, a brief summary of the model design and application will be presented. More details can be found in the original study (Van Vliet et al., 2011).

2.4.2 Available datasets

Several datasets were used for this study. A worldwide dataset of river temperatures was available from the United Nations Environment Programme Global Environment Monitoring System (GEMS/Water; http://www.gemswater.org/). For river discharge, daily mean and monthly mean series for stations on a global scale were available from the Global Runoff Data Centre (GRDC; http://grdc.bafg.de/). In our study, river temperature and discharge data series have been used from 157 stations globally (see Figure 2.6 and Table 2.4), for which both water temperature data from GEMS/Water and discharge data from GRDC were available over the period 1980-1999. In addition to the GEMS/Water data, a second dataset was compiled that consists of daily water temperature and river discharge series for 14 stations in 13 river basins (mainly USA, Europe and Russia) This data was provided by different data sources. The location of these study basin stations, GEMS/Water stations and the number of water temperature measurments for the 1980-1999 period is shown in Figure 2.6.

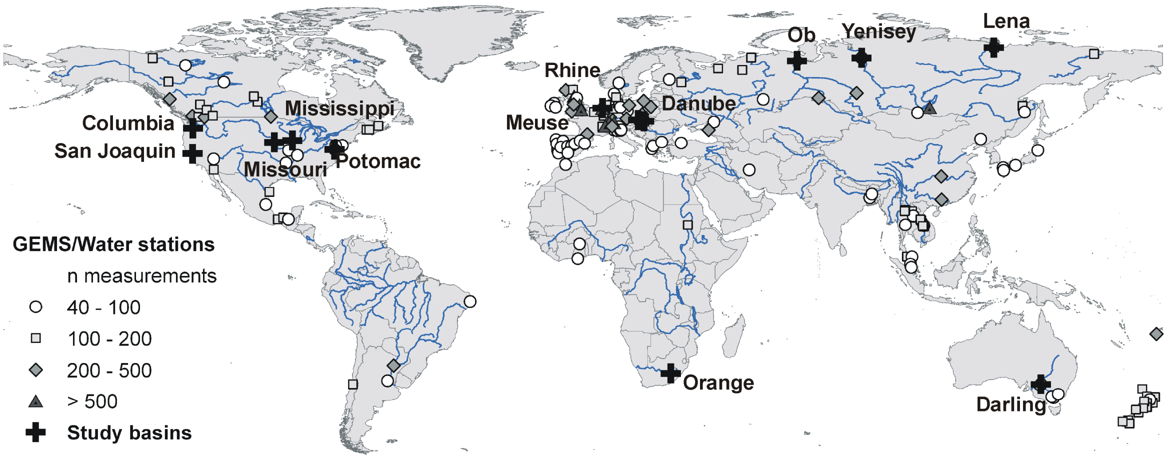

Figure 2.6: Number of measurements for selected GEMS/Water stations for the 1980-1999 period and location of the study basin stations.

Table 2.4: Overview of the total number of GEMS/Water stations, percentage of stations with a small (< 6000 km²), moderate (6000 - 75000 km²) and large (> 75000 km²) upstream basin area, and mean number of water temperature measurements of the selected GEMS/Water stations per region

Region	GEMS/water stations (n)	percentage stations with upstream basin area			mean n per station
		< 6000 km²	6000 - 75000 km²	> 75000 km²	
North America	28	21%	36%	43%	135
South America	4	0%	50%	50%	111
Europe	74	27%	39%	34%	227
Africa	3	0%	33%	67%	66
Asia	25	24%	32%	44%	101
Oceania	23	70%	22%	9%	138
Globally	**157**	**31%**	**35%**	**34%**	**171**

A third dataset consisted of daily temperature and river discharge measurements for the Rhine, Meuse and Danube rivers in the period 2000-2005, provided by the Dutch water management agency (http://live.waterbase.nl) and the Slovak Hydrometeorological Institute, respectively.

For surface air temperature, we used the global gridded 0.5 º x 0.5 º meteorological data set developed within the WATCH project [*Weedon et al., 2010*]. Daily (24 hour) mean air temperature for the 1980-1999 period was extracted from the 0.5 º x 0.5 º grid cells where the study basin and global GEMS/Water stations are located. In addition, daily mean air temperature from the meteorological stations Twente and Maastricht (reference for the Rhine and Meuse River border stations, respectively) provided by KNMI (http://www.knmi.nl/klimatologie/daggegevens/) and Vienna (Danube River; http://eca.knmi.nl/) were used for the period 2000-2005.

2.4.3 Concept of nonlinear water temperature regression model

The regression model in our study is based on the approach of *Mohseni et al.* [1998], who developed a nonlinear regression model, representing the S-shaped function between air temperature and water temperature, to calculate mean weekly stream temperature for monitoring stations in the United States. Modifications to the regression model have been made to include discharge as a variable in addition to air temperature, and to apply the model on a daily time step. An inverse relation between discharge and water temperature was added to the regression model, reflecting higher warming rates under lower discharges as demonstrated in previous studies [*e.g. Rivers-Moore and Jewitt*, 2007; *van Vliet and Zwolsman*, 2008]. Hence, the modified nonlinear regression model used in our study is:

$$Tw = \mu + \frac{\alpha - \mu}{(1 + e^{\gamma(\beta - Tair)})} + \frac{\eta}{Q} + \varepsilon \qquad (1)$$

with: $\gamma = \dfrac{4\tan\theta}{\alpha - \mu}$

Where: μ = lower bound of water temperature (ºC); α = upper bound of water temperature (ºC); γ = measure of the slope at inflection point (steepest slope) of the S-shaped relation ($ºC^{-1}$); β = air temperature at inflection point (ºC); η = fitting parameter ($ºC\ m^3s^{-1}$); *Tw* = water temperature (ºC); *Tair* = air temperature (ºC); *Q* = discharge (m^3s^{-1}); ε = error term (ºC); *tan* θ = slope at inflection point (-).

In addition, a function was included to relate the measure of slope (γ) at the inflection point to the discharge variability compared to the variability in water temperature.

$$\gamma_Q = \gamma(\tau \frac{\sigma_Q}{\sigma_{Tw}}) \qquad (2)$$

Where: γ_Q = measure of slope for discharge term ($ºC^{-1}$); σ_Q = standard deviation of discharge (m^3s^{-1}); σ_{Tw} = standard deviation of water temperature (ºC); τ = fitting parameter ($ºC\ m^{-3}s^{1}$).

The function generally increases the explained variance and sensitivity to air temperature and discharge changes, especially for monitoring stations with a relatively high discharge variability.

To apply the model on a daily basis, a lag effect was incorporated into the regression analyses as water temperature variations tend to lag behind air temperature fluctuations at short timescales (hourly, daily basis) [*Erickson and Stefan*, 2000; *Webb et al.*, 2003], because of the high thermal inertia of water. For the majority of river stations, the optimal time lag was estimated by calculating correlation coefficients between water temperature, air temperature and discharge.

2.4.4 Model performance for the GEMS and study basins stations

For all (14) selected study basin stations, the mean annual cycle of calculated daily water temperatures with the modified regression model including discharge (NONLIN_Q) represents the observed water temperature regime more realistically than those calculated without discharge (NONLIN). Furthermore, the underestimation of water temperatures during summer and overestimation during winter is generally less for NONLIN_Q compared to NONLIN (not shown here; for details see Van Vliet et al., 2011).

Although the number of water temperature measurements for the selected GEMS/Water stations to fit the regression models was generally less than that for the study basin stations, the nonlinear regression models NONLIN and NONLIN_Q were successfully applied to the selected GEMS/Water stations globally. For 126 stations with daily discharge data, the regression models were fitted and the performance was tested on a daily basis, according to the same procedure as for the study basin stations. For 31 GEMS/Water stations with only monthly mean discharge series available, the models were fitted and the performance was tested on a monthly basis. The model performance (efficiency and quality of fit) was determined for both NONLIN and NONLIN_Q by calculating the Nash-Sutcliffe coefficient (NSC) [Nash and Sutcliffe, 1970] and root mean square error (RMSE) [Janssen and Heuberger, 1995]. Non-parametric Wilcoxon Rank Sum tests were performed on the calculated *NSC* and *RMSE* values to test whether the difference between the performance of NONLIN and NONLIN_Q was significant. Results showed that incorporation of discharge (and time lag) led to a statistically significant ($p < 0.01$) improvement of the performance of the water temperature regression model. The increase in the performance of the regression model, reflected by higher values of *NSC* and lower values of *RMSE* for NONLIN_Q compared to NONLIN, was found for 87 % of the GEMS/Water stations. The strongest improvements were found for rivers characterized by typical low flow conditions during summer and high flow conditions during winter or early spring (i.e., the Ohio, Elbe, Rio Usumacinta and Waikato Rivers). For rivers with a peak in discharge during the period with high water temperatures, like the Yangtze, Amur, Kolyma and Mekong, less distinct or no improvements were found by introducing discharge as additional variable into the regression model (Van Vliet et al., 2011).

2.4.5 Model performance during European heat wave of August 2003

The validity of the regression models and parameter estimates for the Rhine (Lobith), Danube (Bratislava) and Meuse (Eijsden) was tested specifically for the heat wave and drought of August 2003 (Figure 2.7). Both regression models showed an underestimation of river temperatures, especially during the period when water temperatures are highest (end of July and first two weeks of August). This is due to an underestimation of the defined upper bound of water temperature (α) of the nonlinear regression model of *Mohseni et al.* [1998], which has also been discussed by *Bogan et al.* [2006] and *Mohseni et al.* [1999, 2002]. However, introduction of discharge into the regression model resulted in a strong decrease in the underestimation of the modelled water temperatures during this warm, dry period. The mean underestimation by NONLIN_Q compared to NONLIN during July-August 2003 is 0.9 ºC versus 3.0 ºC for the Rhine, 1.3 ºC versus 3.4 ºC for the Danube and 0.4 ºC versus 1.4 ºC for the Meuse. In addition, a distinct improvement in model performance was reflected by great decreases in *RMSE* of 1.9 ºC for the Rhine, 2.0 ºC for the Danube and 0.7 ºC for the Meuse. In fact, the improvement of model performance is much more pronounced during low flow conditions and heat waves (when water temperatures may exceed ecological and cooling purpose thresholds) than under average hydrological conditions.

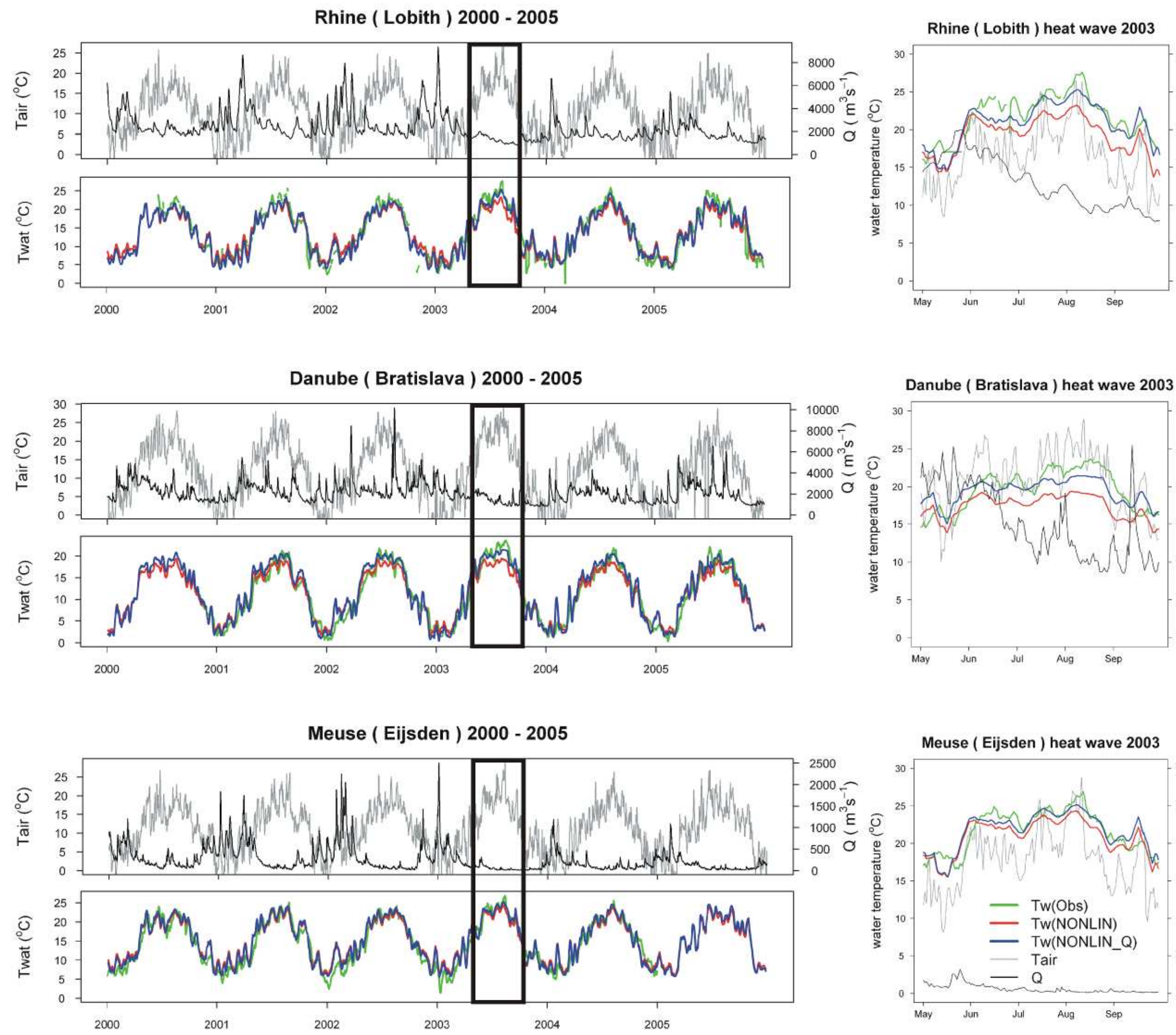

Figure 2.7: Observed daily water temperatures and simulated daily water temperatures for the original regression model [Tw(NONLIN)] and for the adapted regression model including discharge variations [Tw(NONLIN_Q)] for the Rhine (Lobith), Danube (Bratislava) and Meuse (Eijsden) during the validation period 2000-2005, and during the heat wave and summer drought of the 2003. The figures at the right side present the results in more detail during the 2003 heat wave.

2.4.6 Sensitivity of river temperature to changes in air temperature and river discharge

For all study basin stations, annual mean water temperatures were found to increase linearly under air temperature rises (see Table 2.5). A rise in air temperature of +2 ºC results in an annual mean increase of water temperature by 1.5 °C (range: 1.2 to 1.8 ºC). Similarly, a 4°C increase in air temperature results in an average annual increase in water temperature of 2.9 °C (2.2 to 3.6 ºC) and a 6 °C rise in air temperature leads to a 4.2 °C rise (3.1 to 5.3 ºC) in water temperature. Considering the sensitivity of water temperature to discharge changes, an increase in discharge of +20 % generally reduced water temperature rises, while a decrease of 20 % and 40 % in discharge intensified water temperature rises for the majority of river stations (see Table 2.5). This partly reflects the higher thermal capacity of a river under increased river discharges and lower thermal capacity when river discharges are reduced.

Table 2.5: Mean annual river temperature rise (°C) under different air temperature rises and changes in river discharge for study basin stations.

river	station	+ 2 ° C	+ 4 ° C	+ 6 ° C	+ 4 ° C +20 % Q	+ 4 ° C -20 % Q	+ 4 ° C -40 % Q
Columbia	The Dalles	1.2	2.3	3.4	1.6	3.4	5.2
Mississippi	Clinton	1.5	3.0	4.5	3.0	3.1	3.2
Missouri	Omaha	1.4	2.8	4.1	3.1	2.4	1.7
Potomac	Washington D.C.	1.8	3.6	5.3	3.3	3.9	4.5
San Joaquin	Vernalis	1.6	3.0	4.4	2.9	3.2	3.6
Danube	Bratislava	1.3	2.6	3.8	2.4	2.8	3.2
Danube	Budapest	1.5	2.9	4.4	2.7	3.3	3.8
Meuse	Eijsden	1.7	3.3	4.8	3.2	3.4	3.6
Rhine	Lobith	1.7	3.4	5.0	3.1	4.0	4.9
Orange	Oranjedraai	1.1	2.2	3.1	2.3	2.1	1.9
Darling	Burtundy	1.7	3.2	4.6	3.3	3.1	2.9
Ob	Salekhard *	1.2	2.3	3.4	2.3	2.3	2.3
Yenisey	Igarka *	1.3	2.5	3.6	2.2	3.0	4.0

* Stations fitted on 10-daily mean basis instead of daily basis

In order to get more detailed insight into the sensitivity of river temperature on a daily basis, density plots are presented for the San Joaquin (near Vernalis), Potomac (near Washington D.C.), Rhine (Lobith) and Danube (Bratislava), showing the distribution of daily water temperatures under an air temperature rise of +4 ºC, +6 ºC and under an air temperature rise of +4 ºC in combination with a decrease in discharge of 40 % (Figure 2.8). Although the increase in mean annual water temperature is highest under an air temperature rise of +6 ºC, the density plots for these stations indicate that an air temperature rise of +4 ºC in combination with a decrease in discharge of 40 % results in higher maximum water temperatures than found for a single air temperature rise of +6 ºC. The impact of a discharge decrease of 40 % is most pronounced for the Rhine (Lobith), resulting in a considerably higher maximum (99th percentile) water temperature of 28.6 (27.0) ºC, compared to 25.5 (24.6) ºC under an air temperature rise of +4 ºC, and 26.0 (25.0) ºC under an air temperature rise of +6 ºC without any discharge change. As a result, the mean number of days per year that the threshold of 23 °C for the intake of cooling water by thermal power plants [EEA, 2008b] is exceeded, is 16 days for the current climate, 47 days and 83 days under an air temperature rise of + 4 ºC and + 6 ºC respectively, and 104 days per year under an air temperature rise of + 4 ºC in combination with a 40% decrease in river discharge. Although this is a rough estimation, it emphasizes the relevant contribution of decreasing discharges (reduced thermal capacity) to water temperature rises on a daily time step, and the associated impacts for cooling water purposes and aquatic ecosystem functioning.

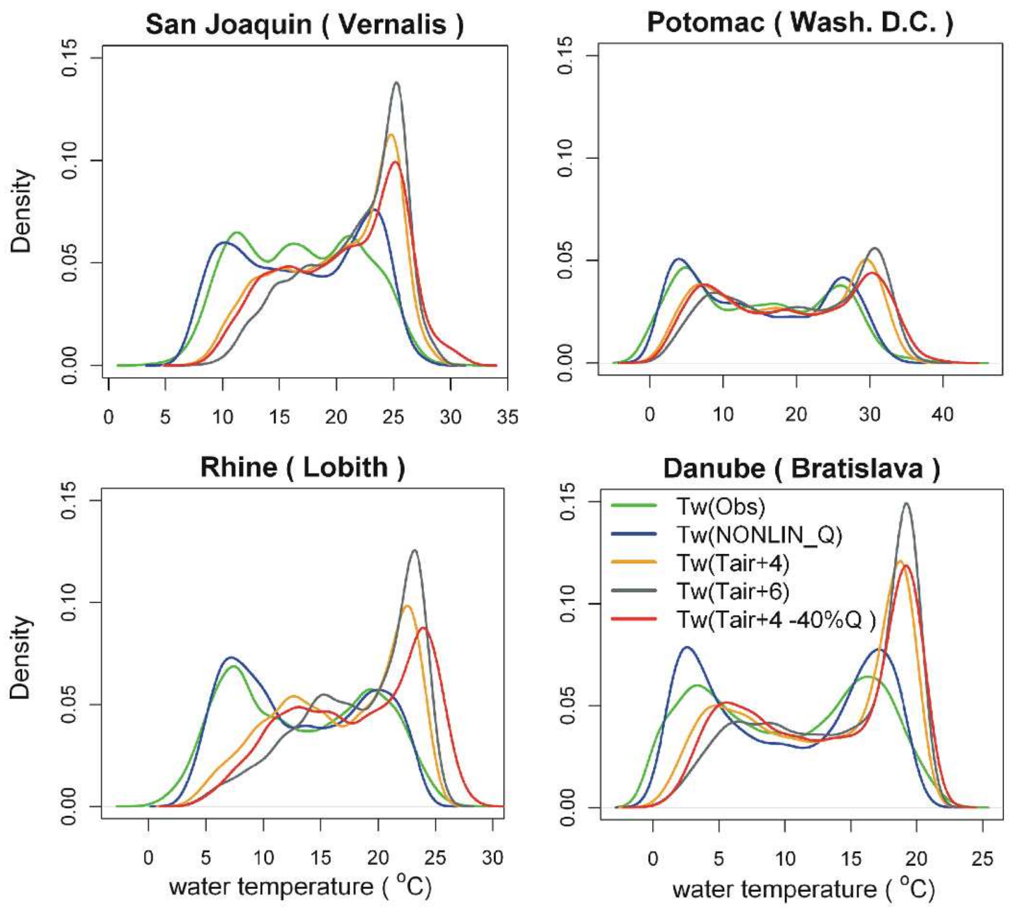

Figure 2.8: Density functions of observed daily water temperature [Tw(obs)] and simulated daily water temperature for the regression model including discharge for the reference period 1980-1999 [Tw(NONLIN_Q)] and under an air temperature rise of +4 °C, +6 °C and under an air temperature rise of +4 °C in combination with a decrease in discharge of 40 %.

2.4.7 Conclusions

The outcomes of our study demonstrate that a nonlinear regression model with air temperature, river discharge and time lag included, is a simple and robust method to estimate river temperatures on a daily basis for monitoring stations in different river basins globally. The performance of the regression model improved for 87 % of the global GEMS/Water river stations where discharge was introduced as an additional variable. Results showed that the impact of discharge changes generally increases during dry, warm periods, when rivers have a lower thermal capacity and are thus more sensitive to warm atmospheric conditions. This high sensitivity of daily water temperatures to discharge changes during dry (low flow) and warm spells is important, as water temperatures can reach critically high values for freshwater ecosystems and several usage functions (e.g. cooling for thermal power plants and industries, drinking water production, recreation) during these periods. Impacts of river discharge on water temperatures should thus be incorporated to provide more accurate estimates of high river temperatures during historical and future projected droughts and heat waves.

3 Water for utilities

3.1 Background

Across Europe as a whole, water is relatively abundant with a total freshwater resource of around 2 270 km^3 /year (EEA, 2009). Only 13 % of this resource is abstracted, suggesting that there is sufficient water available to meet society's demand. In many locations, however, overexploitation by a range of economic sectors poses a threat to Europe's water resources and demand often exceeds availability. As a consequence, problems of water scarcity are widely reported, with reduced river flows, lowered lake and groundwater levels and wetlands drying out as clearly visible symptoms. This general reduction of water resources also has a detrimental impact upon aquatic habitats and freshwater ecosystems. Furthermore, water quality problems may arise during low river flows, due to a reduction of the dilution capacity of rivers and streams. Last but not least, saline intrusion of coastal aquifers (many of which are overexploited) is occurring increasingly throughout Europe, diminishing their quality and preventing subsequent use of the groundwater.

Historically, the problems of water scarcity have been most acute in southern Europe and while this is generally still the case the spatial extent and severity of water stress is growing in parts of the north, too. The impacts of water scarcity are likely to be exacerbated in the future, with predicted increases in the frequency and severity of droughts, driven by climate change. In this chapter, water demand, water availability and water stress will be presented on a European scale, both for the current situation (1971-2000) and the time horizons 2050 (2036-2065) and 2085 (2071-2100). The future projections are based on the socio-economic A2 and B1 scenarios and three global climate models. The SRES scenarios are based on the following storylines:

A2. The A2 scenario describes a very heterogeneous world. The underlying theme is self-reliance and preservation of local identities. Fertility patterns across regions converge very slowly, which results in continuously increasing population. Economic development is primarily regionally oriented and per capita economic growth and technological change more fragmented and slower than in other scenarios.

B1. The B1 scenario describes a convergent world with the same global population, which peaks in the mid century and declines thereafter, with rapid change in economic structures toward a service and information economy, with reductions in material intensity and the introduction of clean and resource efficient technologies. The emphasis is on global solutions to economic, social and environmental sustainability, including improved equity, but without additional climate initiatives.

The storylines in the scenarios were translated to development perspectives for each water consuming sector (domestic, industrial, power production), except for agriculture. Most of the driving forces for the future projections, such as GDP, population density, and thermal electricity production, were provided by IIASA. Other assumptions, like technological and structural changes, were taken from the socio-economical scenario GEO-4. For the A2 scenario we used the assumptions from the Security First scenario, for B1 those from Policy First. As GEO-4 is a global scenario assessment with some regional details, continental differences are not always given.

Security First: People become increasingly preoccupied with fears of a multi-dimensional global catastrophe (e.g. natural disasters, disease pandemics, international terrorism). The government sector and certain private sector actors compete for control in efforts to improve, or at least maintain, human well-being for selected groups.

Policy First: Strong policy constraints are placed on market forces in order to minimize undesirable effects on humans and the environment. The government sector, with active private and civil sector support, implements strong policies intended to improve the environment and human well-being for all, while still emphasizing economic development.

3.2 Water Demand

In the next paragraphs, (future) water demand for domestic use, industrial manufacturing, and thermal power production will be presented, but not for agricultural and ecological purposes. Water demand for agriculture, which is the main consumer in southern Europe, is addressed in another WATCH report (Water for food). To put the figures into perspective, it should be noted that the total abstraction of freshwater across Europe (EU-27) is around 288 km^3/year which represents, on average, 500 m^3 per capita/year (EEA, 2009). Overall, 44 % of the total volume abstracted is used for thermal energy production, 24 % for agriculture, 21 % for public water supply and 11 % for industry. However, strong regional variations occur. In Eastern countries, the greatest abstractor is the electricity generation sector (> 50 %), followed by public water supply (20 %). In western countries, abstraction for electricity production also predominates, contributing approximately 52 % to total abstraction, followed by public water supply (29 %) and industry (18 %). In southern countries, the largest abstraction of water is for agricultural purposes, specifically irrigation, which typically accounts for about 60 % of the total volume abstracted, rising to 80 % in certain locations (EEA, 2009).

Across Europe as a whole, surface water is the predominant source of freshwater, mainly because it can be abstracted easily, in large volumes and at relatively low cost. It therefore accounts for 81 % of the total water volume abstracted. Virtually all abstraction for energy production and more than 75 % of water abstracted for industry and agriculture comes from surface water. However, groundwater's role as a source for agriculture is probably underestimated in southern countries due to uncontrolled (illegal) abstraction by wells. Groundwater is the predominant source (about 55 %) for public water supply due to its generally higher quality than surface water, and because it may be a more reliable source than surface water in the summer months (EEA, 2009).

3.2.1 Domestic water withdrawal

Public water supply accounts for 21% of total water abstraction in Europe, although significant variation exists between countries. Public water not only includes the supply to households but also to small businesses, hotels, offices, hospitals, schools and some small industries. On average, only 20 % of the water used by the various sectors receiving a public water supply is actually consumed, the remaining 80 % being returned to the environment primarily as treated wastewater (EEA, 2003). Urbanization can, however, lead to a depletion of groundwater resources, because groundwater is often a key source of public water supply, whilst augmentation of groundwater stocks in urban areas is limited as most of the rainfall is directed to sewer networks rather than infiltrating in the soil. Moreover, effluents from urban wastewater treatment plants are generally returned to surface water. The key drivers influencing public water demand are population and household size, income, consumer behaviour and tourist activities. Technological developments, including the degree to which leakage in the public water supply system is controlled, also play an important role (EEA, 2009).

Domestic water withdrawals in Europe were calculated for the present and future situation, based on (projected) population times water usage per capita (water intensity), which in turn is related to GDP per capita development. Details on the calculations and underlying assumptions are provided in WATCH Technical report no. 46 (Flörke and Eisner, 2011).Behavioral changes as well as water savings due to technological developments were considered in the calculations. The results are shown in Figures 3.1 (population density), 3.2 (water use per capita) and 3.3 (total domestic water consumption).

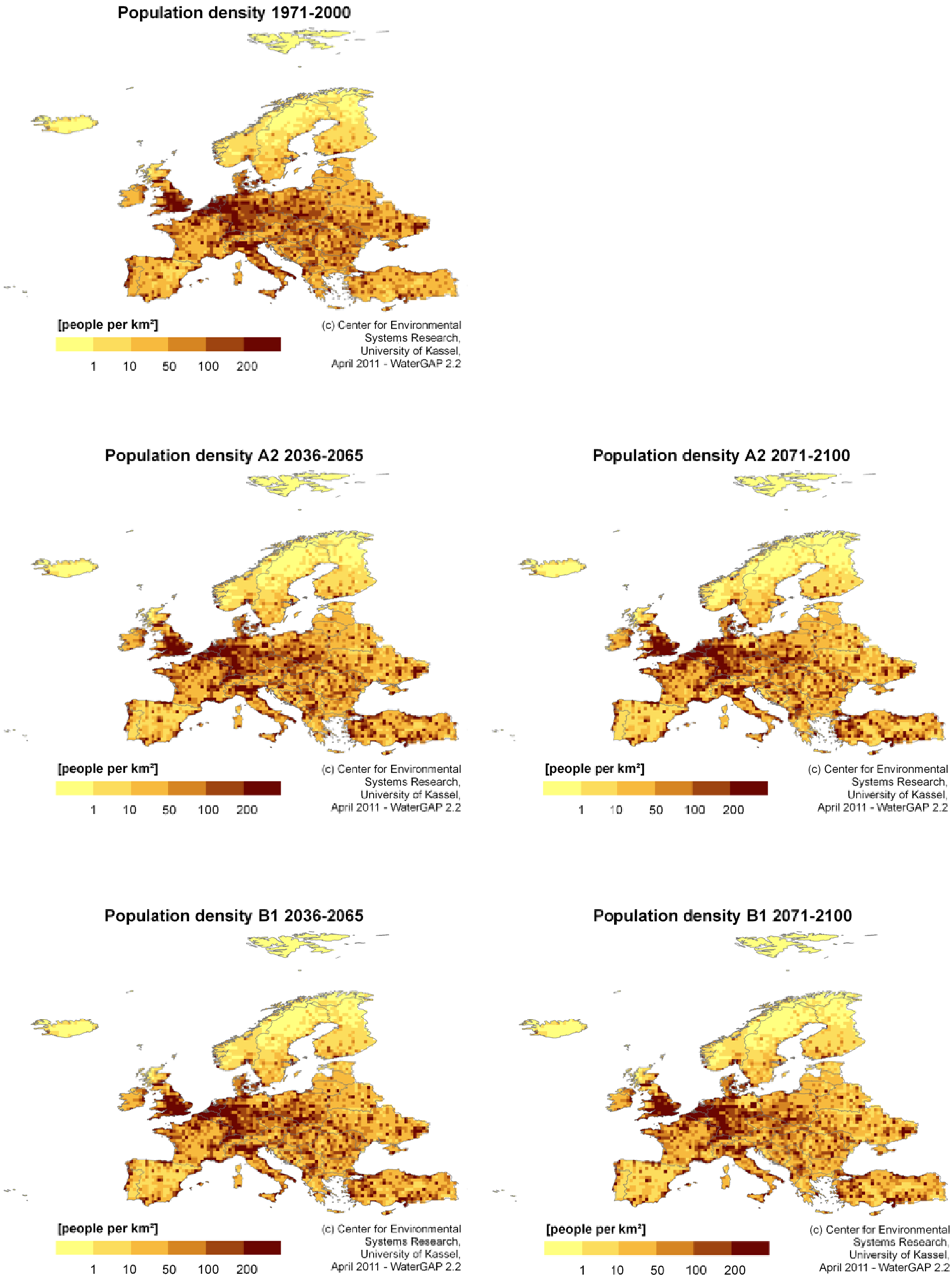

Figure 3.1. Present and future population density in Europe, according to the A2 and B1 scenarios.

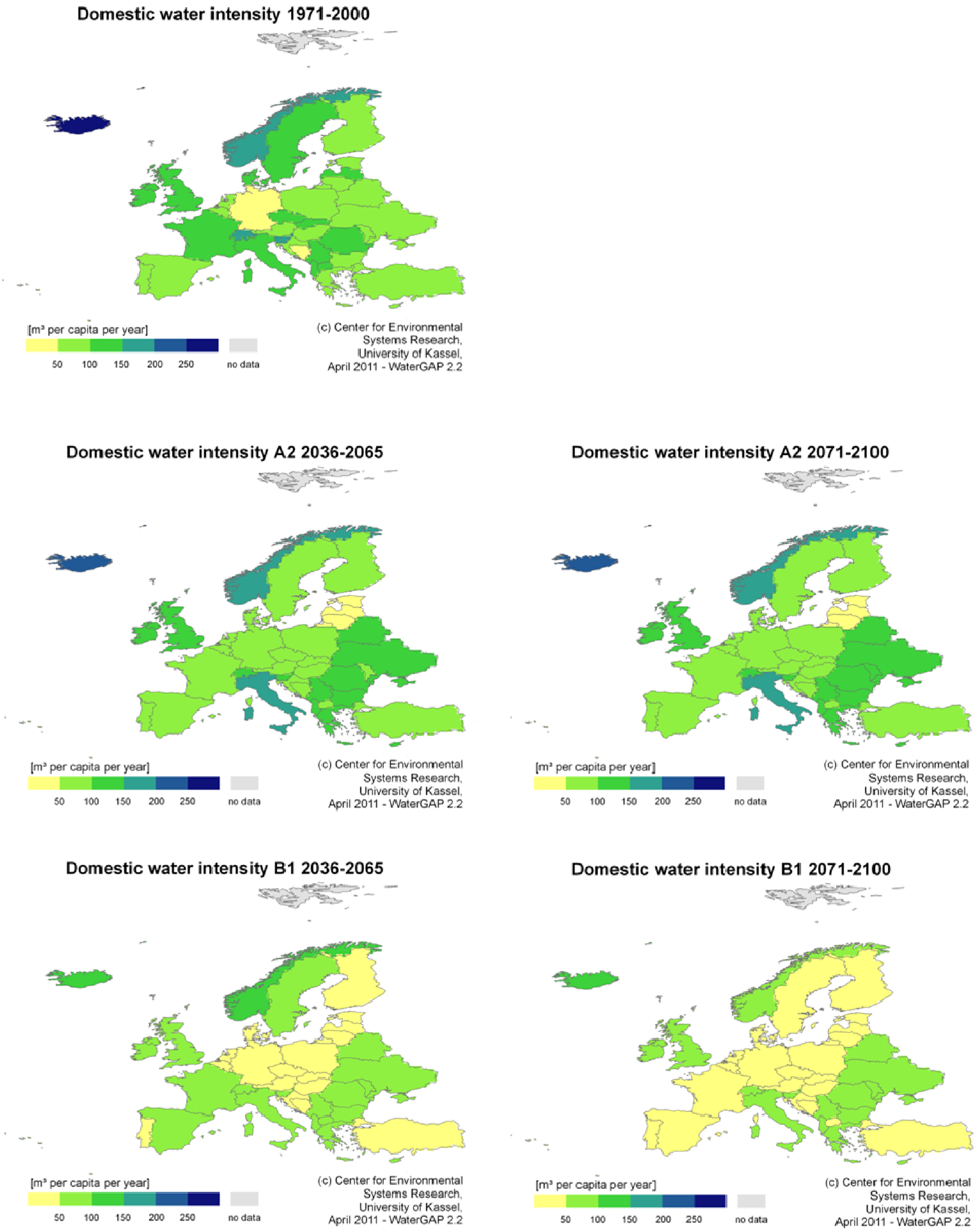

Figure 3.2. Present and future domestic water use per capita in Europe, according to the SRES A2 and B1 scenarios.

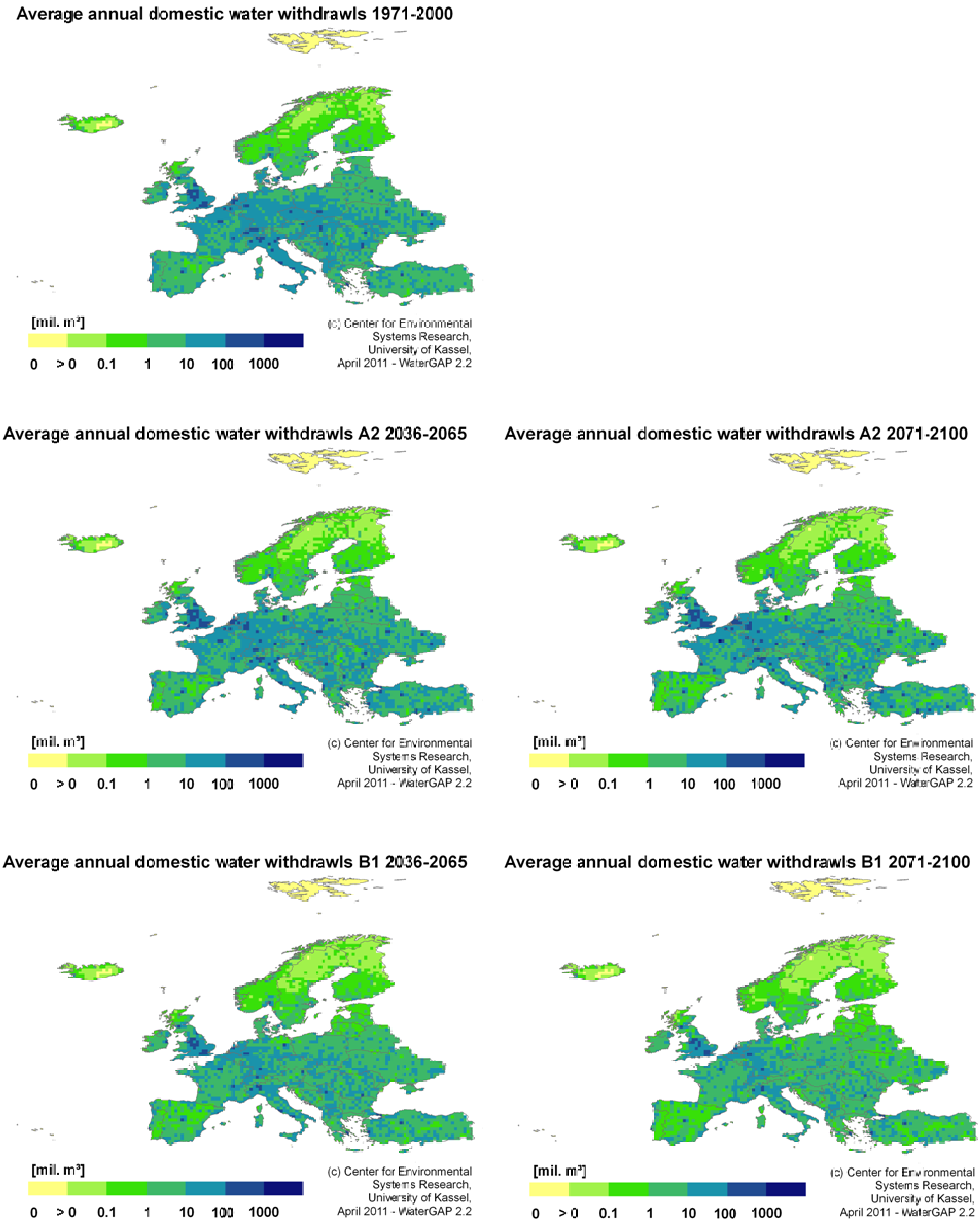

Figure 3.3. Present and future annual domestic water withdrawal in Europe, according to the SRES A2 and B1 scenarios.

The main characteristics of these figures can be summarized as follows.

Fig. 3.1: In general, the highest population density is observed in North-west Europe, e.g. southern England, Belgium (Flanders), the Netherlands and western Germany (Ruhr area). Another densely populated area is the Po river plain in northern Italy. Isolated hot spots on the maps represent big cities like Madrid, Paris, Berlin, Athens etc. In the year 2050, both the A2 and B1 scenarios project a higher number of people in northern Europe (+13%) and western Europe (+7%), a decreasing population in southern Europe (-7%) and eastern Europe (-12%), and a very strong population growth in Turkey (+39% to +58%; see Table 3.1). For the year 2085, the scenario projections differ strongly. In the A2 scenario (2085), a further increase in population occurs in northern Europe (+13% compared to 2050) and western Europe (+11% compared to 2050), whilst the population further decreases in southern Europe (-7% compared to 2050) and eastern Europe (-7% compared to 2050). In the B1 scenario (2085), the population stabilizes in northern Europe (+2% compared to 2050) and western Europe (-2% compared to 2050) and a dramatic decrease of the population is projected in southern Europe (-22% compared to 2050) and eastern Europe (-26% compared to 2050). In Turkey, the population increases further under the A2 scenario (+8% compared to 2050) but decreases strongly under the B1 scenario (-15% compared to 2050).

Table 3.1. Current and future population of Europe (million people) under the SRES A2 and B1 scenarios

	2000	**2050 (A2)**	**2050 (B1)**	**2085 (A2)**	**2085 (B1)**
Europe (all regions)	647.1	677.0	671.1	702.1	589.4
Northern Europe	93.9	106.2	106.1	120.5	107.9
Western Europe	183.0	195.2	195.5	215.9	191.4
Southern Europe	145.3	134.1	135.9	125.2	106.5
Eastern Europe (central)	64.4	59.6	62.7	56.2	46.7
Eastern Europe (eastern)	94.4	77.7	79.3	71.8	58.7
Turkey	66.0	104.1	91.7	112.6	78.3

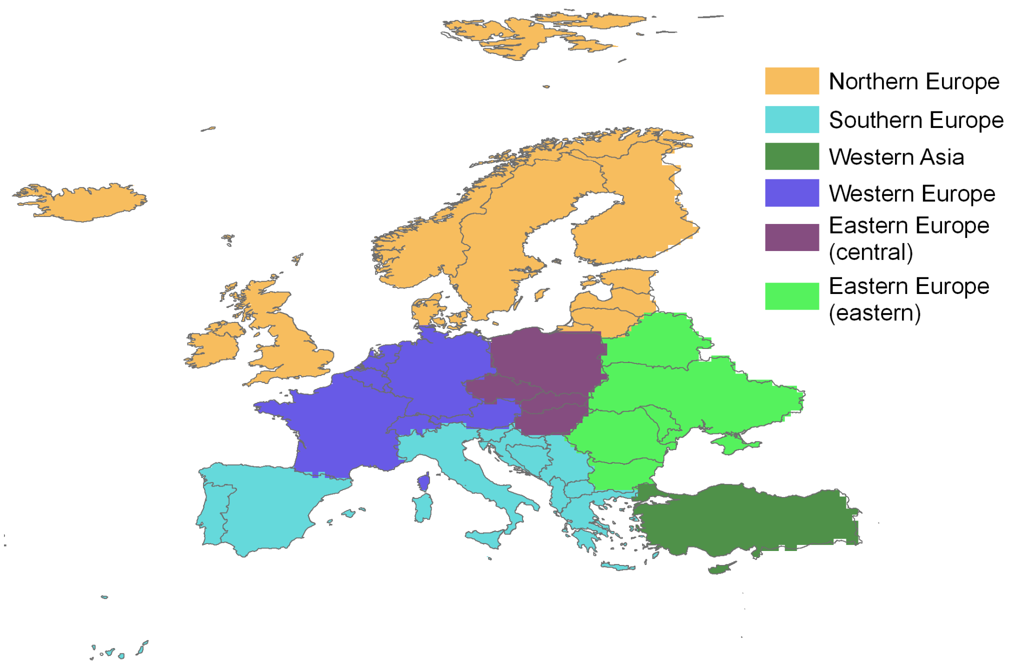

Figure 3.4. European regions referred to in Tables 3.1 to 3.4.

Fig. 3.2: The current domestic water intensity was based on average values for the period 1971-2000, mostly taken from national statistics. A remarkable result is the extremely high water use per capita in Iceland, which is related to the use of geothermal freshwater for heating (included in the calculations). In Norway, Switzerland and Slovenia, the domestic water intensity is also relatively high. In the A2 scenario, domestic water intensity increases in several countries (e.g. Germany, Italy, Eastern Europe), yet decreases in others (e.g. France, Switzerland, the Baltic countries). After 2050, no further changes are projected. On the one hand, these developments are related to an increase in GDP per capita, leading to an increase in water use intensity in households (more water-intensive appliances, e.g. power showers). On the other hand, technological progress will lead to a slight decrease of domestic water use intensity (projected as 0.25% per year up to 2025, then stand still up to 2100). In the B1 scenario a general tendency towards a decreasing domestic water intensity across whole Europe can be observed (but less so in eastern Europe), which continues up to the year 2100. This trend is due to technological improvement accompanied by an increasing public commitment to save water.

Fig. 3.3: By combining the maps of population density and domestic water intensity, maps of average annual domestic water withdrawals were constructed. The blue spots in these maps represent the larger cities and agglomerations in Europe. A marked difference can be observed between future domestic water withdrawals under the A2 and B1 scenarios, reflecting the difference in domestic water intensity due to water savings (in 2050), partially also the different population densities (in 2085). The resulting domestic water withdrawals under the A2 and B1 scenarios are summarized in Table 3.2.

Table 3.2. Current and future annual domestic water withdrawals in Europe (km^3/yr)

	1971-2000	2050 (A2)	2050 (B1)	2085 (A2)	2085 (B1)
Europe (all regions)	56.5*	65.5	39.2	66.4	30.3
Northern Europe	10.9	12.7	7.7	13.9	6.6
Western Europe	13.3	16.0	9.7	17.3	8.1
Southern Europe	14.2	15.4	9.5	14.2	6.6
Eastern Europe (central)	5.6	4.3	2.8	4.0	1.9
Eastern Europe (eastern)	8.8	9.1	5.4	8.5	3.9
Turkey	3.5	7.9	4.2	8.4	3.2

* 60.5 km^3/yr according to EEA (2009)

In the A2 scenario (2050), an increase in domestic water withdrawals is projected in western Europe (+20%), northern Europe (+16%), southern Europe (+8%) and eastern Europe (+4%), whilst in central eastern Europe a decrease (-23%) is projected. It is anticipated that the European water suppliers will be able to deal with these figures. In Turkey, however, the domestic water withdrawals are projected to more than double in 2050 (A2), which will put a major challenge to local water supply infrastructure. In the B1 scenario, the trend is just the opposite, featuring a strong decline in domestic water withdrawals all over Europe in 2050: northern Europe -30%, western Europe -27%, southern Europe -34%, eastern Europe -43%. Only in Turkey an increase in domestic water withdrawals is projected (+18%), but much less as in the A2 scenario.

In the period 2050-2085, only modest changes in domestic water withdrawals occur in the A2 scenario. Domestic water withdrawals slightly increase in northern Europe, western Europe and Turkey (by 7-10%), and slightly decrease in southern Europe and eastern Europe (-7% compared to 2050). In the B1 scenario, a further decrease in domestic water withdrawals occurs between 2050-2085, typically by 15% in northern and western Europe, by 30% in southern and eastern Europe, and by 23% in Turkey.

3.2.2 Manufacturing water witdrawals

Water is used by manufacturing industries in a number of different ways: for cleaning, heating and cooling; to generate steam; as a transport medium; as a raw material; as a solvent; and as a constituent part of the product itself (e.g. in the beverage industry). Overall, the manufacturing industry uses about 11 % of the total freshwater volume abstracted across Europe, about half of which used for processing and the remainder for cooling (EEA, 2009). The manufacturing industry is supplied both from the public water supply system and by self abstraction; the more water-intensive industries generally abstract raw water by themselves, mainly from surface water. The various manufacturing sectors account for differing proportions of total industrial water use in Europe. Data reported to Eurostat indicate that the chemicals and petroleum refinement industries are responsible for approximately half of all water abstracted by the manufacturing industry, while the basic metals, paper and food processing industries account for much of the remainder. Just two countries, Germany and France, account for more than 40% of the European water abstraction by the manufacturing industry (EEA, 2009).

The present and future average annual water withdrawals by the European manufacturing industry are shown in Figure 3.5 and summarized in Table 3.3. Industrial withdrawals are high in Flanders, the Netherlands, the Ruhr area and northern Italy. Several other hot spots can be observed on the map. A dramatic increase in industrial manufacturing water abstraction is projected in the A2 scenario, e.g. in western Europe (+28% in 2050) and northern Europe (+35% in 2050), but especially in central Eastern Europe (+275% in 2050) and Turkey (+686% in 2050), reflecting the rapid industrialization in these regions anticipated in the coming decades. Between 2050-2085, the growth continues all over Europe, leading to an overall 74% increase in water abstraction by the manufacturing industry in Europe in the A2 scenario compared to the reference situation (1971-2000). By contrast, the B1 scenario projects a continuous decrease in industrial water abstraction, due to increasing technological efficiency, except for central eastern Europe and Turkey, where industrial growth predominates. As a consequence, the projected overall abstraction by the European manufacturing industry decreases in the B1 scenario by 17% in the year 2050 and by another 17% in the year 2085 compared to the reference situation.

Table 3.3. Current and future annual manufacturing water withdrawals in Europe (km^3/yr)

	1971-2000	2050 (A2)	2050 (B1)	2085 (A2)	2085 (B1)
Europe	58.8*	78.5	48.8	102.5	38.6
Northern Europe	7.6	10.3	6.7	12.4	5.2
Western Europe	20.0	25.6	16.8	29.7	11.5
Southern Europe	17.9	19.2	11.8	22.9	7.8
Eastern Europe (central)	2.1	7.7	4.7	11.5	5.7
Eastern Europe (eastern)	10.2	8.1	4.9	10.7	4.0
Turkey	0.97	7.6	3.9	15.4	4.5

* 31.7 km^3/yr according to EEA (2009)

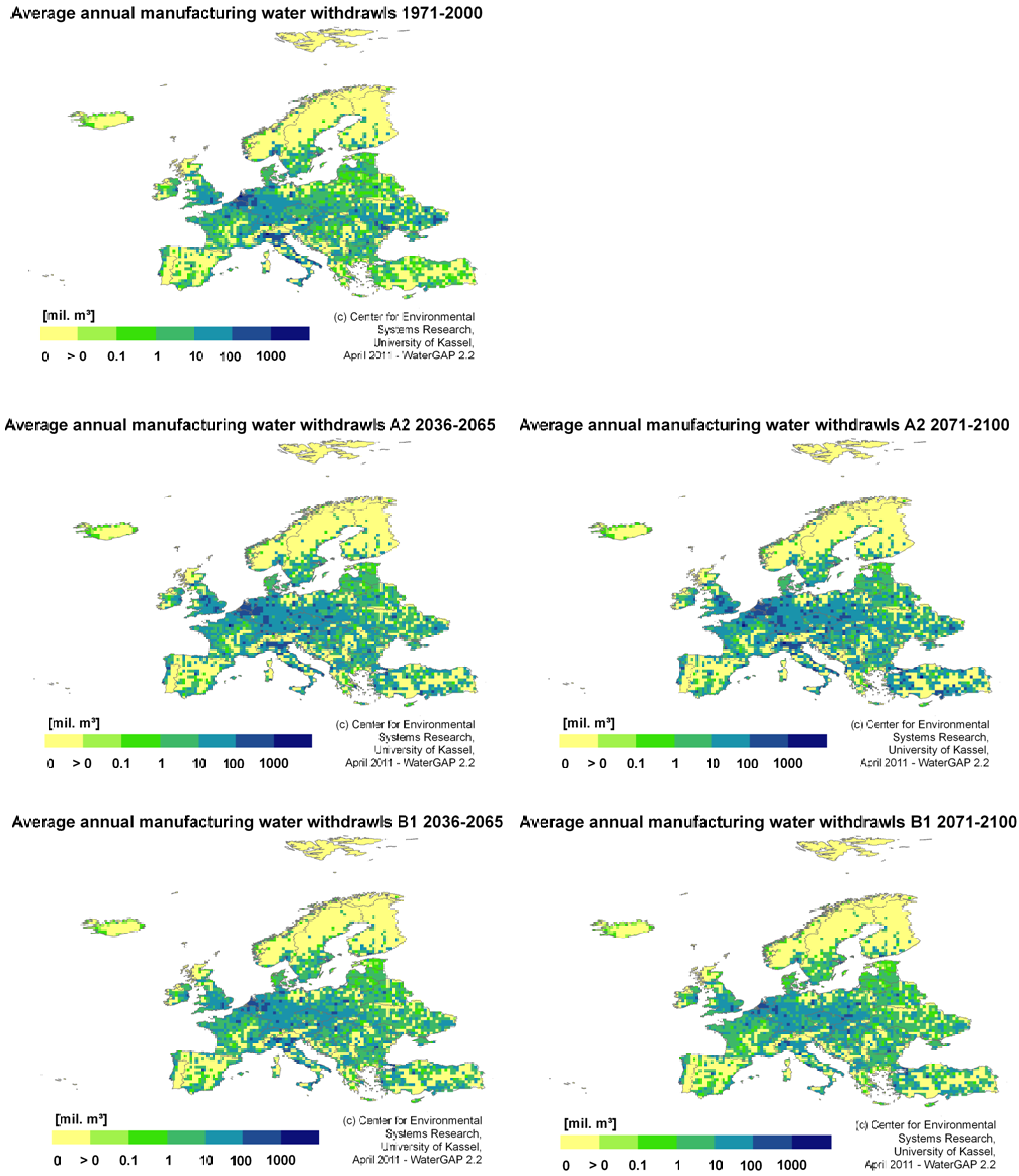

Figure 3.5. Present and future annual manufacturing water withdrawal in Europe, according to the SRES A2 and B1 scenarios.

3.2.3 Water withdrawal for electricity production

Water abstracted for energy production accounts for about 44 % of the total freshwater abstracted across Europe, although in Germany, France and Poland this figure exceeds 50 %. Very little water abstracted for energy production is truly consumed, with the majority ultimately discharged back to a receiving water body at a higher temperature. Thermal power plants (either based on fossil fuels, biomass or nuclear energy) all require large amounts of water for the generation of electricity and heating. The water abstracted is used primarily for cooling, although some is used as 'boiler feed' and 'process' water. Most of the water requirements of power plants are met by surface water and extracted almost exclusively by self-owned abstraction plants. Cooling water is generally treated with different chemicals in order to avoid corrosion and calcification and also to control the growth of bacteria and algae in the cooling system (EEA, 2009).

The present and future annual water withdrawals for electricity production in Europe are shown in Figure 3.6, and the related cooling water discharges in Figure 3.7. As more than 90% of the water needed for cooling is returned to surface water, the maps for water withdrawals and cooling water discharges are virtually the same. At present, high water withdrawals can be found all over Europe (except Scandinavia, where most of the electricity is produced by hydropower), however most of the hot spots are situated in western Europe and central eastern Europe.

An overview of present and future water withdrawals for electricity production is presented in table 3.4. In the A2 scenario (2050), a dramatic decrease in water withdrawals for electricity is projected in western Europe (- 80%) and central eastern Europe (- 67%). Smaller changes are projected in northern Europe (-26%) and eastern Europe (-15%). In southern Europe, however, an increase in abstractions for electricity is projected in 2050 (+47%). In the B1 scenario, a dramatic decrease in water withdrawals for electricity is projected all over Europe, occurring largely in the coming decades. The main reason for these trends is a change in cooling type of the power plants from once-through cooling to tower cooling (consuming much less water). Under the A2 scenario, it was assumed that after a 50 years lifetime all once-through cooling systems in the EU30 countries are replaced by tower cooling. Although thermal electricity production does increase in the A2 scenario, the extra water withdrawals are dwarfed by the transition to tower cooling. In the B1 scenario, it was assumed that tower cooling would be implemented after a plant lifetime of 35 years for all European countries. Moreover, in the B1 scenario electricity production by thermal power plants decreases due to increasing wind and solar sources. Consequently, a much stronger decrease in water abstraction for electricity production is projected in the B1 scenario compared to the A2 scenario.

Table 3.4. Current and future water withdrawals for electricity production in Europe (km^3/yr)

	1971-2000	**2050 (A2)**	**2050 (B1)**	**2085 (A2)**	**2085 (B1)**
Europe	166.7*	91.7	7.7	74.9	3.3
Northern Europe	11.0	8.1	0.84	2.1	0.35
Western Europe	82.7	16.9	2.1	8.2	1.6
Southern Europe	19.6	28.8	2.1	24.2	0.56
Eastern Europe (central)	15.4	5.2	0.91	3.2	0.41
Eastern Europe (eastern)	36.3	30.9	1.5	36.5	0.25
Turkey	1.6	1.8	0.18	0.61	0.12

* 127 km^3/yr according to EEA (2009)

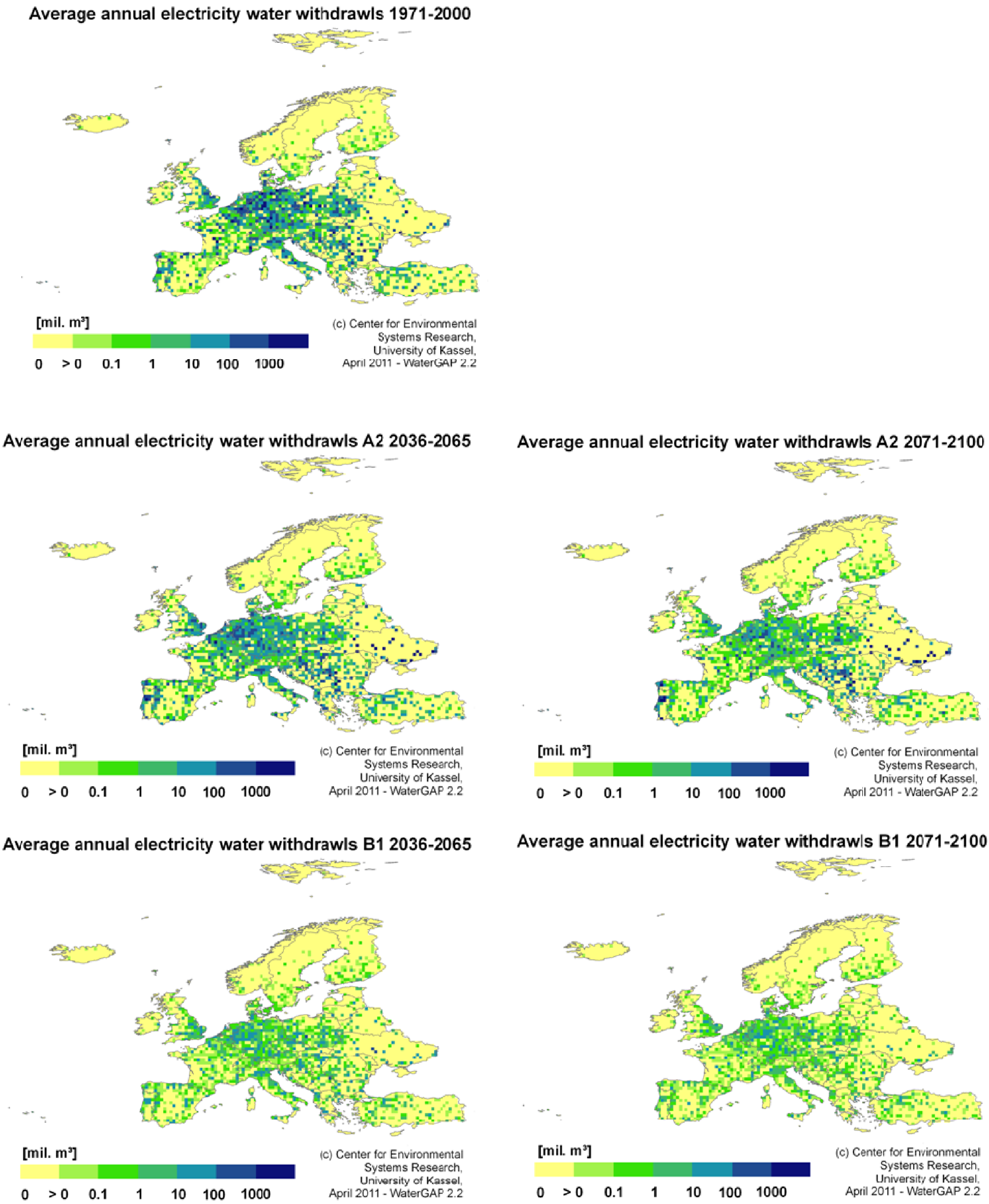

Figure 3.6. Present and future water withdrawals for electricity production in Europe, according to the SRES A2 and B1 scenarios.

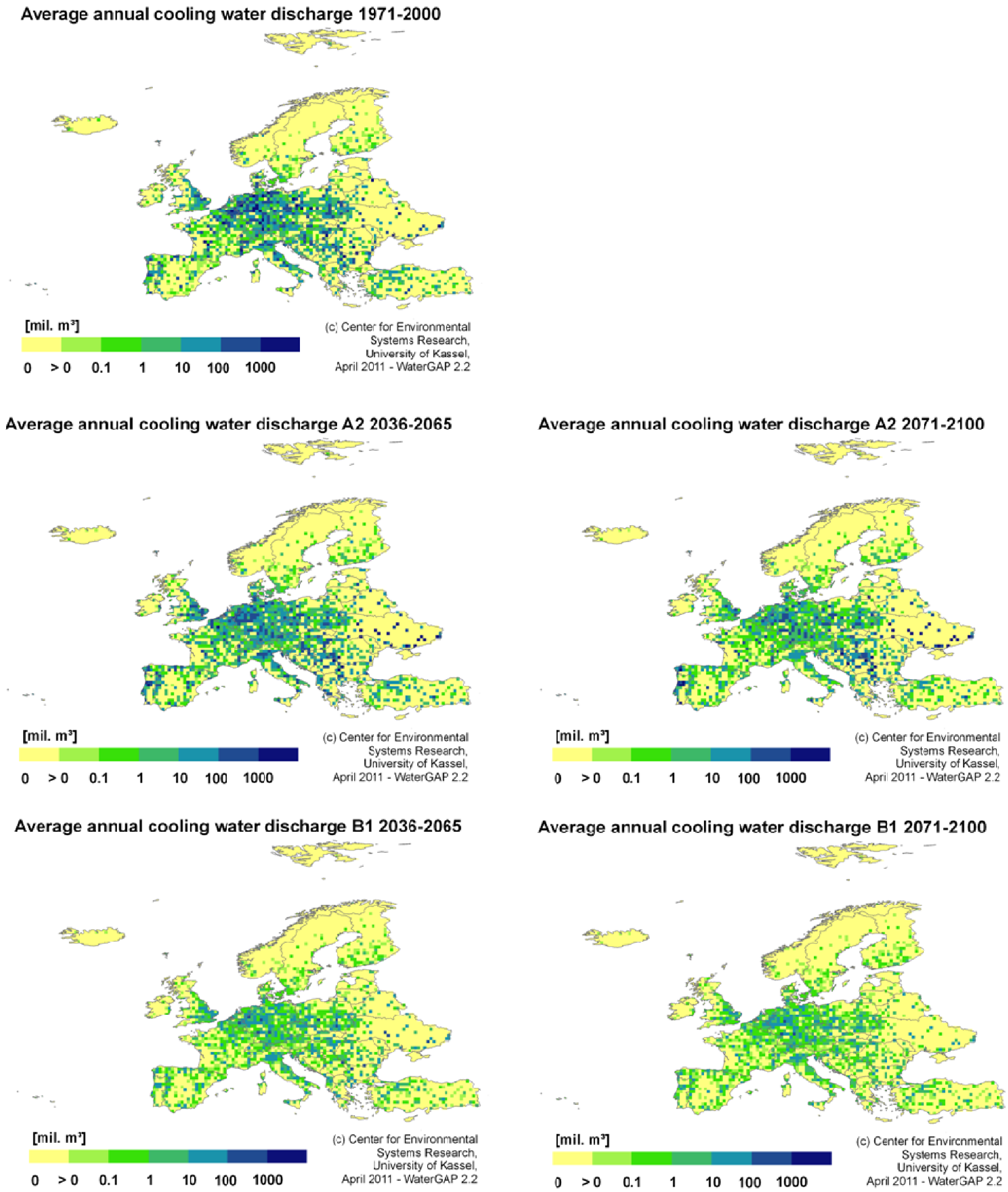

Figure 3.7. Present and future cooling water discharges related to electricity production in Europe, according to the SRES A2 and B1 scenarios.

3.3 Water availability

Changes in river discharge in Europe for the 2050s (2041-2060) and 2080s (2071-2100) have been assessed using the Variable Infiltration Capacity (VIC) macro-scale hydrological model [*Liang et al.*, 1994], which was applied on daily time step and on 0.5° x 0.5° spatial resolution. In a first step, the performance of the VIC model was assessed by comparing the daily river discharge simulations for the observed WATCH forcing data [*Weedon et al.*, 2010; *Weedon et al.*, submitted] during the period 1971-2000 with observed daily river discharge for more than 1500 river stations globally. In a next step, VIC was forced with bias corrected output of three different GCMs (CNCM3, ECHAM5, IPSL) for both the SRES A2 and B1 scenarios [*Hagemann et al.*, 2011; *Piani et al.*, 2010]. Simulations were performed for the control period 1971-2000 and for the future periods 2041-2060 and 2071-2100. The spatial patterns of projected changes in mean river discharge, low flows and high flows for these future periods relative to the control period are shown in Figure 3.8. These changes in flow statistics are presented for both the A2 and B1 scenarios, and were calculated by using the average daily river discharge series for the three different GCMs. Changes in low river flow were assessed by calculating the relative changes in the river discharge exceeded 90% of the time (Q90) between the future periods and control period. High river flow was defined as the river discharge exceeded 5% of time (Q5).

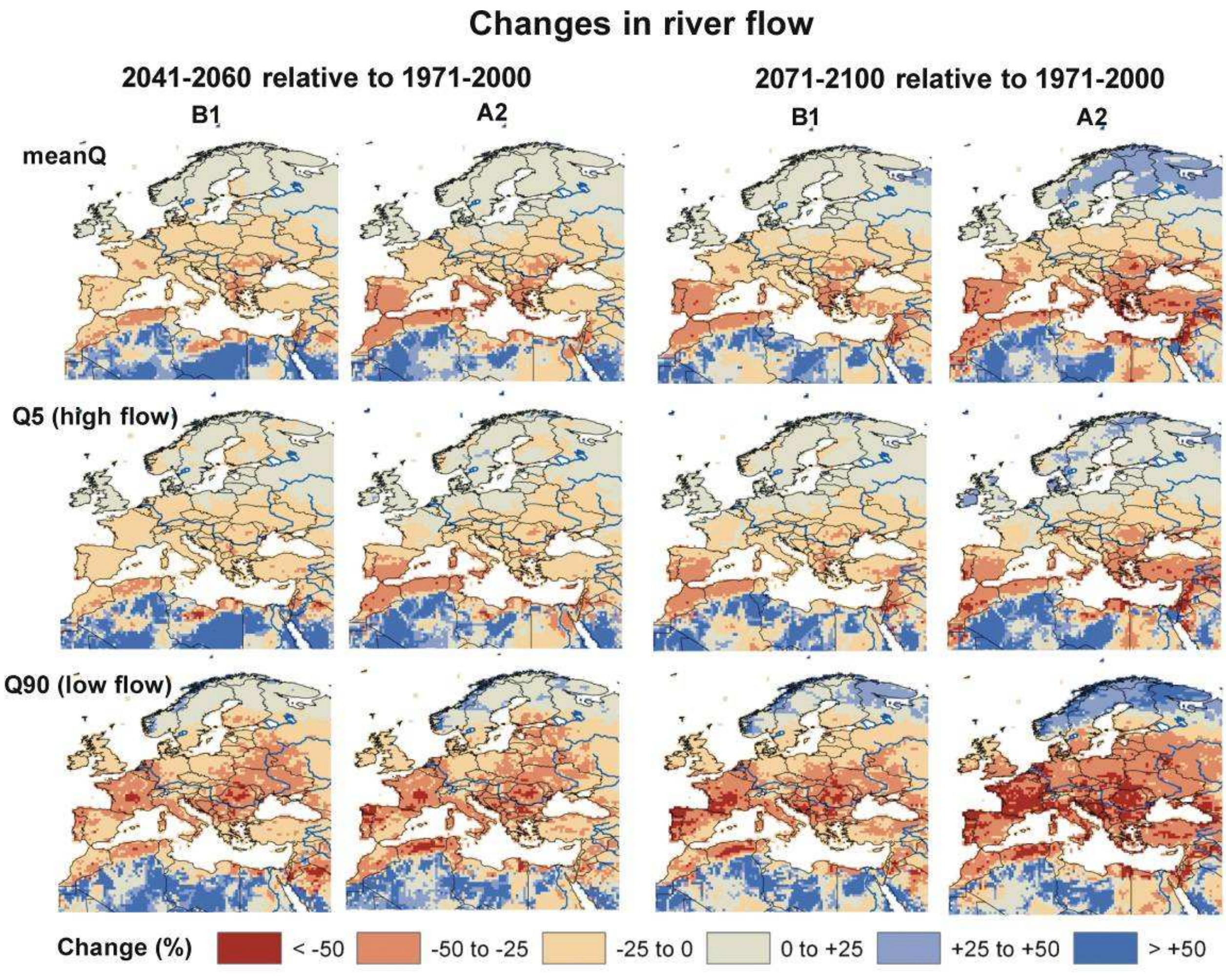

Figure 3.8. Simulated relative changes in mean annual river discharge, high flow and low flow in Europe for the 2050s (2041-2060) and 2080s (2071-2100). The spatial pattern of projected changes in river discharge were calculated based on daily river discharge projections produced with the hydrological model VIC, for three different GCMs (CNCM3, ECHAM5, IPSL) under the SRES A2 and B1 scenario.

Considering the changes in mean river flows (upper panels of Figure 3.8), a general decrease in water availability is projected for most of Europe, except the northern part (Scandinavia, UK, Ireland), with the largest effects occurring in southern Europe (e.g. Portugal, Spain, Italy, Greece) and eastern Europe (e.g. Bulgaria, Rumania, Turkey). Moreover, impacts are stronger for the A2 than for the B1 scenario, although spatial trends are similar for both scenarios. For northern Europe, however, an increase in river discharge on mean annual basis is projected, especially under the A2 scenario in the 2080s. Similar patterns as for average river flows can be observed for high flows (Q5; middle panels of Figure 3.8) and low flows (Q90; lower panels), but the changes in high flow are relatively small, compared to the large changes projected for the low flow conditions. Under the A2 scenario, large parts of southern and eastern Europe face a decrease of low river flows by 25-50% in the 2050s, and of >50% in the 2080s. In these regions, the low river flow period generally occurs during summer, when the demand of river water for several river functions (e.g. irrigation, energy, drinking water) is generally the highest. In other words, the water scarcity problems which are already manifest in southern and south-eastern Europe (e.g. EEA, 2009), will be strongly amplified by climate change.

3.4 Water stress

3.4.1 The Water Exploitation Index

One relatively straightforward indicator of the pressure or stress on freshwater resources is the water exploitation index (WEI), which is calculated annually as the ratio of total freshwater abstraction to the total renewable resource. A WEI above 20 % implies that a water resource is under stress and values above 40 % indicate severe water stress and clearly unsustainable use of the water resource (Raskin *et al.*, 1997). The WEI is available on a national level and for a growing number of river basins, which better reflects the extent and severity of water scarcity on regional scale. For example, while Spain's national WEI is approximately 34 %, the southern river basins of Andalusia and Segura have extremely high WEIs of 164 % and 127 %, respectively (EEA, 2009).

Although calculating the WEI at a river basin scale provides additional detail, such analysis still fails to fully reflect the level of stress upon local water resources. This is primarily because the WEI is based on annual data and cannot, therefore, account for seasonal variations in water availability and abstraction. During the summer months in southern Europe, for example, agricultural and tourist water demands peak at a time when the natural water resource availability reaches a minimum. The annual average approach of the WEI is unable to capture this and cannot, therefore, fully reflect the potential threat to, for example, the freshwater ecosystem. On the other hand, the WEI can also overestimate water stress because it does not account for the non-consumptive use of water. Where abstraction is dominated by power generation, for instance, nearly all the abstracted water is returned to the source.

Despite its limitations, the WEI still provides a useful indication of water scarcity and there is a broad geographical correlation between river basins with the highest WEI and diminished water resources and associated detrimental impacts, such as drying out of wetlands, ecological damage, seawater intrusion, aquifer degradation, etc. A typical map of (future) water stress in Europe, based on the WEI (including all relevant water consuming sectors), is shown in Figure 3.9.

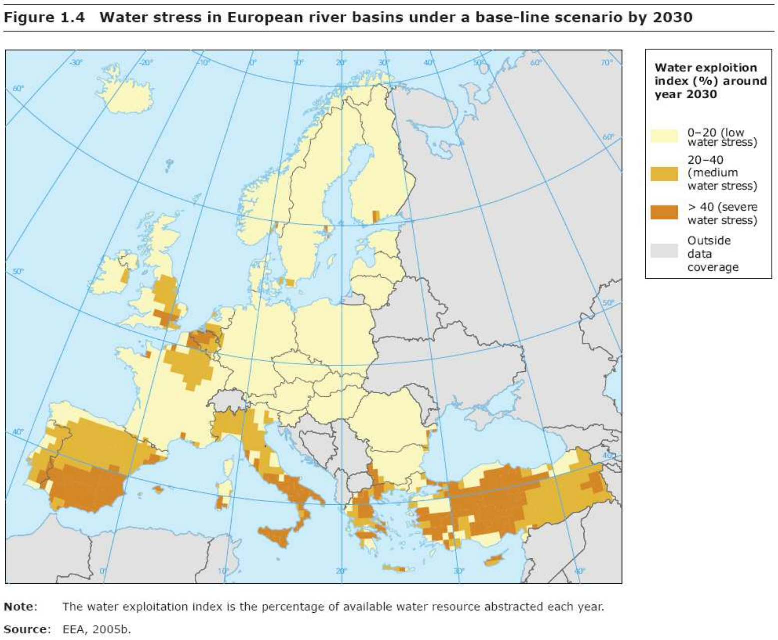

Figure 3.9. Water stress in European river basins under a baseline scenario by 2030 (EEA, 2005)

3.4.2 Assessment of future water stress in Europe

In Figures 3.10 to 3.12, the current and future water stress in Europe is presented and discussed, based on the water withdrawal and water availability assessments described in the paragraphs 3.2 and 3.3. It should be realized that water withdrawals in this study were limited to domestic water supply, industrial production (manufacturing) and electricity generation. Thus, **agricultural water use was not included in the water stress calculations.** This means that the water stress maps presented here only partially reflect the severity of European water stress. Especially in southern Europe, where agriculture is the main water consumer, the water stress situation is much more serious than presented in this study.

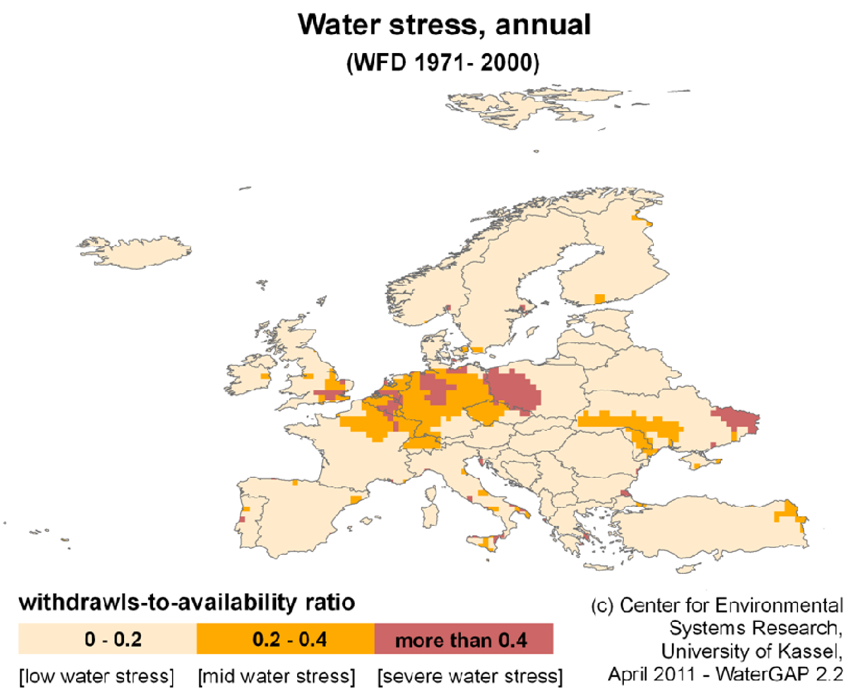

Figure 3.10. Current water stress in Europe according to the WATCH forcing dataset (1971-2000), excluding agricultural water demand.

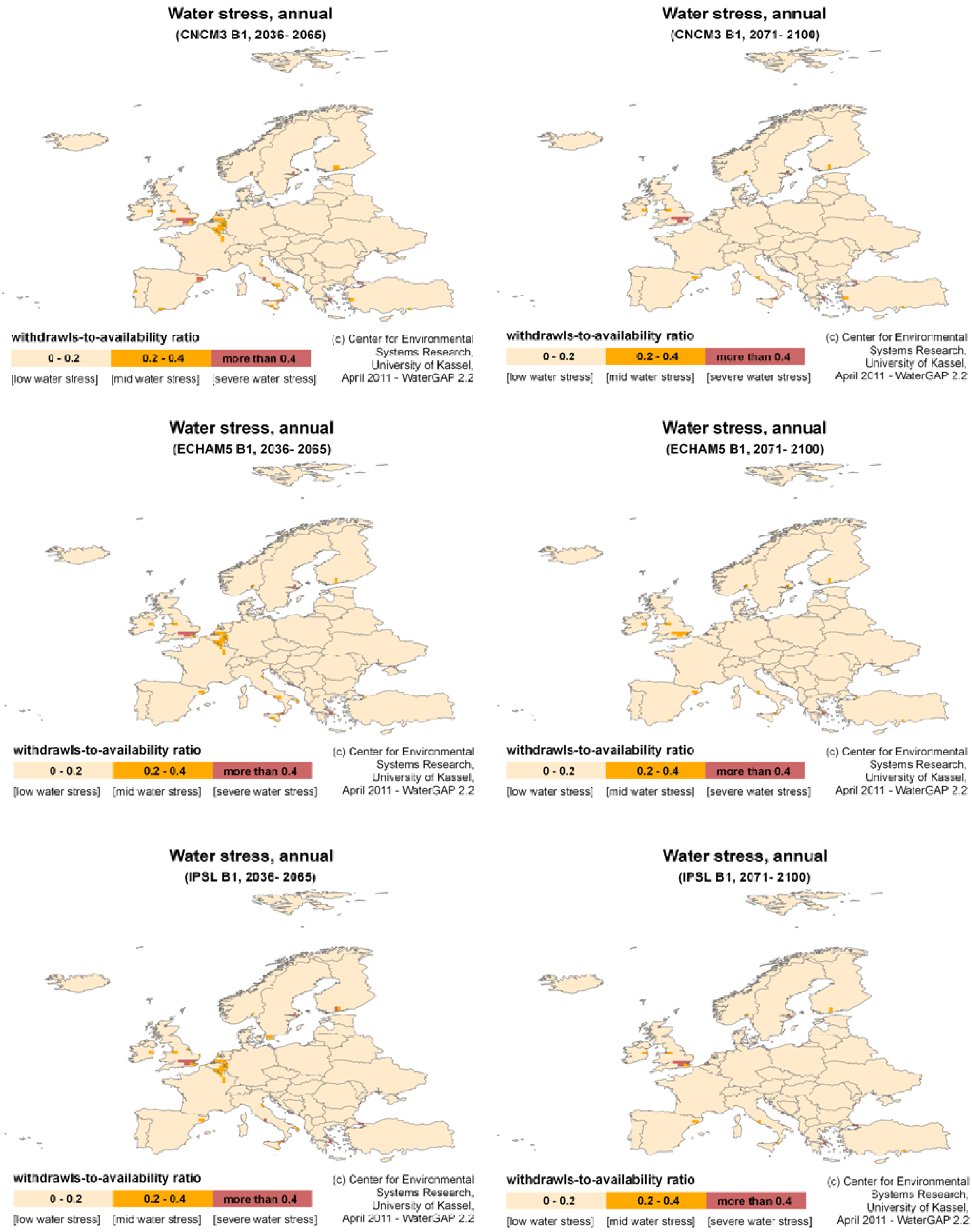

Figure 3.11. Projection of future water stress in Europe around 2050 and 2085 for three different GCMs and the SRES B1 scenario (agricultural water demand not included).

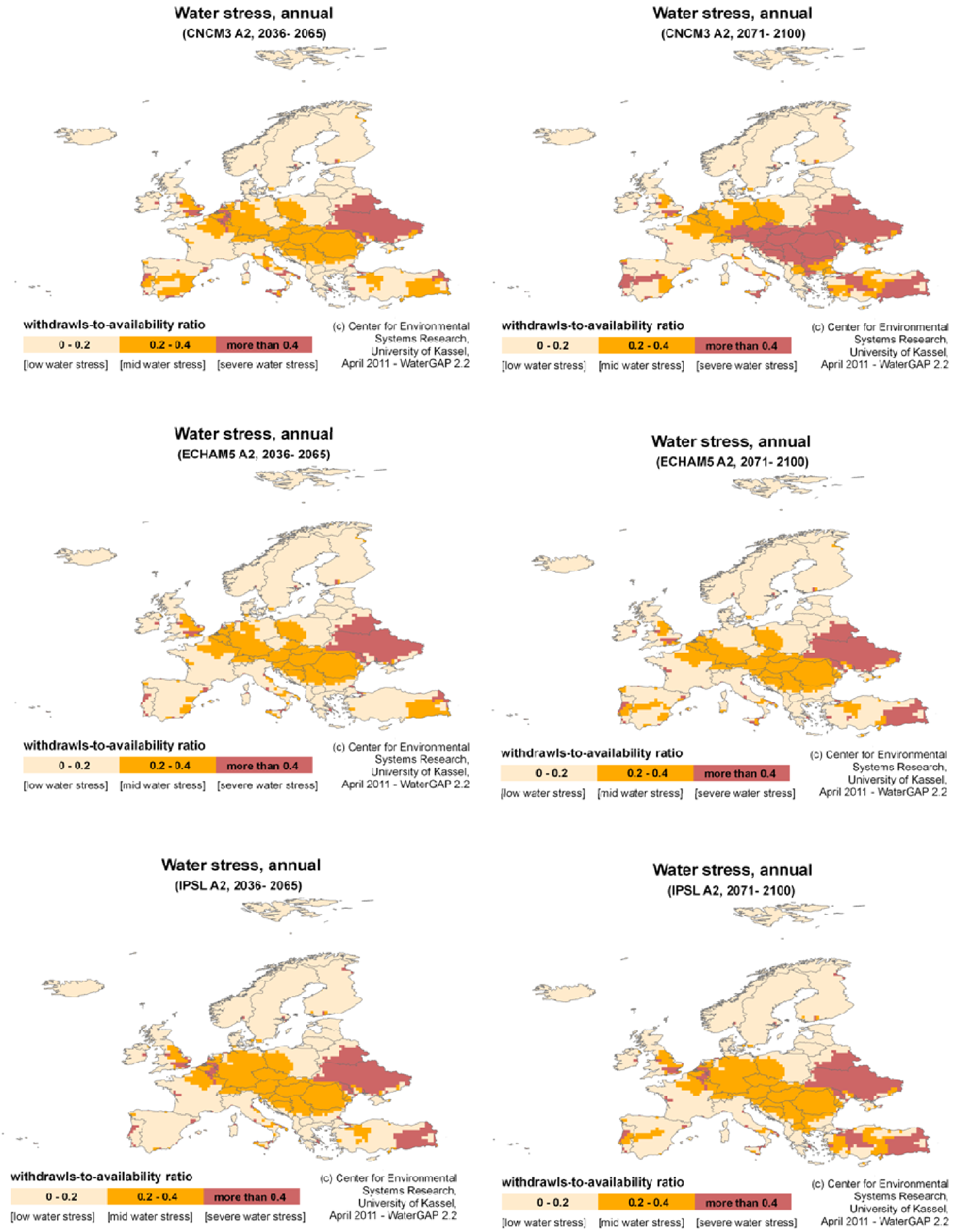

Figure 3.12. Projection of future water stress in Europe around 2050 and 2085 for three different GCMs and the SRES A2 scenario (agricultural water demand not included).

The main observations from these figures are the following:

Fig. 3.10: In the reference situation (1971-2000), water stress mainly occurs in western Europe and central eastern Europe. Hot spots (severe water stress) are observed in eastern Ukraine, western Poland, northern Germany, the southern Netherlands, eastern Belgium and south-western England. Generally, no water stress is observed in Mediterranean countries, but this is certainly due to the fact that agricultural water demand was not considered in the calculations. Based on the water demands of the individual sectors (Table 3.5), it can be assumed that most of the water stress which occurs in the reference situation will be related to water withdrawals by the electricity sector. As most of this water is returned to the water system (albeit with higher temperature), the water stress will be overestimated in many cases, as mentioned before.

Table 3.5: Current water demand of economic sectors in Europe (km^3/yr)

1971-2000	**Dom.**	**Man.**	**Elec.**	**total**
Europe (all regions)	56,5	58,8	166,7	**282**
Northern Europe	10,9	7,6	11,0	**29,6**
Western Europe	13,4	20,0	82,7	**116**
Southern Europe	14,3	18,0	19,7	**51,9**
Eastern Europe (central)	5,6	2,1	15,4	**23,1**
Eastern Europe (eastern)	8,8	10,2	36,3	**55,3**
Turkey	3,5	1,0	1,6	**6,1**

Fig. 3.11: In the B1 scenario, water demand for electricity production has declined dramatically (>95%) because of the transition from once-through cooling to tower cooling. Moreover, water withdrawals for domestic water supply and manufacturing have also decreased between the reference period and the 2050s, and this decrease continues towards the 2080s (Table 3.6). Although water availability also decreases in the same period (Figure 3.8), the decrease in water demand, mainly due to the vanishing need of cooling water, clearly outweighs the lesser water availability. As a result, water stress in the B1 scenario is only locally observed in the future projections, the two major examples being the greater London agglomeration (severe water stress, both in the 2050s and 2080s) and the Meuse River basin (medium water stress in 2050, disappearing in 2085).

Table 3.6: Future water demand of economic sectors in Europe in the SRES B1 scenario (km^3/yr)

B1 scenario	**2050**				**2085**			
	Dom.	**Man.**	**Elec.**	**Total**	**Dom.**	**Man.**	**Elec.**	**Total**
Europe	39,2	48,8	7,7	**95,8**	30,3	38,6	3,3	**72,2**
Northern Europe	7,7	6,7	0,84	**15,2**	6,6	5,2	0,4	**12,1**
Western Europe	9,7	16,8	2,1	**28,6**	8,1	11,6	1,6	**21,3**
Southern Europe	9,5	11,8	2,1	**23,4**	6,6	7,8	0,6	**15,0**
Eastern Europe (central)	2,8	4,7	0,9	**8,4**	1,9	5,7	0,4	**8,0**
Eastern Europe (eastern)	5,5	4,9	1,5	**11,9**	3,9	4,0	0,3	**8,2**
Turkey	4,2	3,9	0,18	**8,3**	3,2	4,5	0,1	**7,8**

Fig. 3.12: In the A2 scenario, medium to severe water stress is projected in western Europe, south-western England, eastern Europe, Turkey, and locally in the Mediterranean. This is mainly due to the decreasing water availability in the future projections (Figure 3.8), as water demand in most European regions decreases (e.g. western Europe) or stabilizes at the reference level (e.g. northern Europe). Only in southern Europe and Turkey, an increase in water demand is projected between the reference period and the future, contributing to the local water stress situation (cf. Table 3.7 and Table 3.5). The severity of water stress is certainly underestimated in southern Europe, as agricultural water demand was not included in the water stress calculations. Nevertheless, medium to severe water stress is projected in the Tagus basin (Spain/Portugal) in the 2080's, even in the absence of agricultural water use!

Table 3.7: Future water demand of economic sectors in Europe in the SRES A2 scenario (km^3/yr)

A2 scenario	**2050**				**2085**			
	Dom.	**Man.**	**Elec.**	**Total**	**Dom.**	**Man.**	**Elec.**	**Total**
Europe	65,5	78,5	91,7	**236**	66,4	102,5	74,9	**244**
Northern Europe	12,7	10,3	8,1	**31,1**	13,9	12,4	2,1	**28,4**
Western Europe	16,0	25,6	16,9	**58,5**	17,3	29,7	8,2	**55,2**
Southern Europe	15,4	19,2	28,8	**63,3**	14,2	22,9	24,2	**61,3**
Eastern Europe (central)	4,3	7,7	5,2	**17,3**	4,0	11,5	3,2	**18,7**
Eastern Europe (eastern)	9,1	8,1	30,9	**48,2**	8,5	10,7	36,5	**55,7**
Turkey	7,9	7,6	1,8	**17,3**	8,4	15,4	0,6	**24,4**

4 Conclusions and recommendations

4.1 Conclusions

4.1.1 Climate change and water quality

Climate change may have a serious impact on the water quality of river systems which are already moderately to strongly polluted, because of the increase of low flow periods (in frequency and intensity) with minimal dilution. This was clearly shown by the relation between chloride concentration and river flow in a number of European rivers. Moreover, seawater intrusion into river mouths is enhanced during low river flows, as shown by the IJsselmeer example in the Netherlands. This may have consequences for drinking water supply, industrial production and agriculture as water quality standards are exceeded.

A nonlinear regression model with air temperature, river discharge and time lag included, has proven to be a simple and robust method to estimate river temperatures on a daily basis globally. Results showed that the impact of changes in river flow generally increases during dry, warm periods, when rivers have a lower thermal capacity and are thus more sensitive to warm atmospheric conditions. This high sensitivity of daily water temperatures to discharge changes during dry and warm spells is important, as water temperatures can cross threshold values for freshwater ecosystems and several usage functions (e.g. cooling for thermal power plants and industries, drinking water production, recreation) during these periods. Impacts of river discharge on water temperatures should thus be incorporated in temperature models to provide more accurate estimates of high river temperatures during droughts and heat waves.

4.1.2 Sectoral water demands

In the A2 scenario (2050), an increase in domestic water withdrawals is projected in western Europe (+20%), northern Europe (+16%), southern Europe (+8%) and eastern Europe (+4%), whilst in central eastern Europe a decrease (-23%) is projected (compared to the reference situation; 1971-2000). It is anticipated that the European water suppliers will be able to deal with these figures. In Turkey, however, the domestic water withdrawals are projected to more than double in 2050 (A2), which will put a major challenge to local water supply infrastructure. In the B1 scenario, the trend is just the opposite, featuring a strong decline in domestic water withdrawals by 30-40% all over Europe in the 2050s. Only in Turkey an increase in domestic water withdrawals is projected (+18%), but much less as in the A2 scenario.

In the A2 scenario, a dramatic increase in industrial manufacturing water abstraction is projected in central Eastern Europe (+275% in 2050) and Turkey (+686% in 2050), due to rapid industrialization in these regions anticipated in the coming decades. Between 2050-2085, the growth continues all over Europe, leading to an overall 74% increase in water abstraction by the manufacturing industry in Europe compared to the reference situation (1971-2000). By contrast, the B1 scenario projects a continuous decrease in industrial water abstraction, due to increasing technological efficiency, except for central eastern Europe and Turkey, where industrial growth predominates. As a consequence, the projected overall abstraction by the European manufacturing industry decreases in the B1 scenario by 17% in the year 2050 and by another 17% in the year 2085 compared to the reference situation.

A dramatic decrease in water withdrawals for electricity production is projected in Europe by 2050, both for the A2 and the B1 scenarios. The main reason for these trends is a change in cooling type of the power plants from once-through cooling to tower cooling (consuming much less water). Under the A2 scenario, it was assumed that after a 50 years lifetime all once-through cooling systems in the EU30 countries are replaced by tower cooling. Although thermal electricity production does increase in the A2 scenario, the extra water withdrawals are dwarfed by the transition to tower cooling. In the B1 scenario, it was assumed that tower cooling is implemented after a plant lifetime of 35 years for all European countries. Moreover, in the B1 scenario electricity production by thermal power plants decreases due to increasing wind and solar sources. Consequently, a quicker and stronger decrease in water abstraction for power production is projected in the B1 scenario compared to the A2 scenario.

4.1.3 Water availability

Climate change projections with three GCMs and two socio-economic scenarios (A2 and B1) indicate that future river discharges will decrease all over Europe, except northern Europe. The largest effects are projected to occur in southern Europe (e.g. Portugal, Spain, Italy, Greece) and eastern Europe (e.g. Bulgaria, Rumania, Turkey). Moreover, impacts are stronger for the A2 than for the B1 scenario. For northern Europe an increase in river discharge is projected, especially under the A2 scenario. Similar observations as for average river flows are projected for high flows (Q5) and low flows (Q90), but the changes in high flow values are relatively small, compared to the large changes projected for low flow conditions. Under the A2 scenario, large parts of southern and eastern Europe face a decrease of low river flows by 25-50% in the 2050s, and of >50% in the 2080s. In the B1 scenario, the decrease in low river flows is smaller, but still significant. In southern Europe, the low river flow period generally occurs during summer, when the demand of river water for several river functions is highest. Therefore, it can be concluded that the water scarcity problems which are already manifest in southern and south-eastern Europe will be strongly amplified by climate change.

4.1.4 Water stress

Water stress In Europe was evaluated based on the Water Exploitation Index, the ratio of total water demand and water availability. Water withdrawals were limited to domestic water supply, industrial production (manufacturing) and electricity generation. Thus, agricultural water use was not included in the water stress calculations. This means that the severity of water stress may be underestimated in many cases, especially in southern Europe, where agriculture is the main water consumer.

In the reference situation (1971-2000), water stress mainly occurs in western Europe and central eastern Europe. Severe water stress is found in eastern Ukraine, western Poland, northern Germany, the southern Netherlands, eastern Belgium and south-western England. Most of the water stress which occurs in the reference situation is related to water withdrawals by the electricity sector. As almost all of this water is returned to the water system as cooling water (albeit with higher temperature), the water stress will be overestimated in many cases.

In the B1 scenario, water demand for electricity production has declined dramatically (>95%) due to the transition from once-through cooling to tower cooling. Moreover, water withdrawals for domestic water supply and manufacturing have also decreased between the reference period and the 2050s, and this decrease continues towards the 2080s. Although water availability also decreases in the same period, the decrease in water demand, mainly due to the vanishing need of cooling water, clearly outweighs the lesser water availability. As a result, water stress in the B1 scenario is only locally observed in the future projections, the two major examples being the greater London agglomeration (severe water stress, both in the 2050s and 2080s) and the Meuse River basin (medium water stress, disappearing in the 2080s).

In the A2 scenario (2050), medium to severe water stress is projected in western Europe, south-western England, eastern Europe, Turkey, and locally in the Mediterranean. This is mainly due to decreasing water availability in the future projections, as water demand in most European regions decreases or at least stabilizes at the reference level (1971-2000). Only in southern Europe and Turkey, an increase in water demand is projected between the reference period and the future, contributing to the local water stress situation. It should be noted that the severity of water stress is certainly underestimated in the Mediterranean region, as agricultural water demand was not included in the water stress calculations.

4.2 Recommendations

In the assessment of water stress, agricultural water withdrawals have been omitted. As a result, the water stress assessment presented in this study underestimates the true severity of European water stress, especially in southern and south-eastern Europe where agriculture often is the dominant water consumer. Therefore, it is recommended to include agricultural water abstraction in the assessment of water stress.

The water stress assessments have been based on average annual values of water withdrawals and water availability. However, there is a strong seasonal influence on water stress. Generally, water stress in southern Europe will be highest in the summer when river flows are generally low and water demand is highest, aggravating the true water stress situation. To capture this phenomenon, it is recommended to perform water stress assessments on a seasonal basis, rather than on an annual average basis.

It was found that water quality (chloride concentration, water temperature) declines during heat waves and low flow conditions. The challenge is to model these water quality parameters in the context of climate change. Due to the apparent relations between chloride concentration and river flow, and water temperature versus air temperature and river flow, it should be possible to use climate forcing data to model these simple, yet important, water quality parameters, on a European and even global scale.

5 References

Bogan, T., J. Othmer, O. Mohseni & H. Stefan (2006). Estimating extreme stream temperatures by the standard deviate method. *Journal of Hydrology* 317: 173-189.

Bonte, M. & J.J.G. Zwolsman. (2010). Climate change induced salinisation of artificial lakes in the Netherlands and consequences for drinking water production. *Water Research* 44: 4411-4424.

Caissie, D. (2006). The thermal regime of rivers: a review. *Freshwater Biology* 51: 1389-1406.

Delpla, I., A.-V. Jung, E. Baures, M. Clement & O. Thomas (2009). Impacts of climate change on surface water quality in relation to drinking water production. *Environment International* 35: 1225-1233.

EEA, 2005. Vulnerability and adaptation to climate change in Europe. EEA Technical report No 7/2005.

EEA (2007). Climate change and water adaptation issues. EEA Technical report No 2/2007.

EEA (2008a). Impacts of Europe's changing climate – 2008 indicator-based assessment. EEA Report No 4/2008.

EEA (2008b). Energy and environment report 2008. EEA Report No 6/2008.

EEA (2009). Water resources across Europe – confronting water scarcity and drought. EEA Report No 2/2009.

EEA (2011). Safe water and healthy water services in a changing environment. EEA Technical report No 7/2011.

Erickson, T.R. & H.G. Stefan (2000). Linear air/water temperature correlations for streams during open water periods. *Journal of Hydrologic Engineering 5:* 317-322.

Flörke, M. & S. Eisner (2011). The development of global spatially detailed estmates of sectoral water requirements, past, present and future, including discussion of the main uncertainties, risks and vulnerabilities of human water demand. WATCH Technical Report No. 46.

Hagemann, S., C. Chen, J. O. Härter, J. Heinke, D. Gerten & C. Piani (2011). Impact of a statistical bias correction on the projected hydrological changes obtained from three GCMs and two hydrology models. *J. Hydrometeor. (in press)*

Hurkmans R., W. Terink, R. Uijlenhoet, P. Torfs, D. Jacob & P.A. Troch (2010). Changes in Streamflow Dynamics in the Rhine Basin under Three High-Resolution Regional Climate Scenarios. J. Climate 23: 679-699.

IPCC (2008). Climate change and water. IPCC Technical Paper VI (B. Bates, Z.W. Kundzewicz, S. Wu & J. Palutikof, eds.). IPCC Secretariat, Geneva, 210 pp.

IWA (2009). Climate change and the water industry – Practical responses and actions. IWA Perspective Document no 10 (J.J.G. Zwolsman & A. Johannesen, eds.). Presented at 5th World Water Forum, Istanbul.

Janssen, P.H.M. & P.S.C. Heuberger (1995). Calibration of process-oriented models. *Ecological Modelling 83:* 55-66.

Krysanova V., F. Hattermann, et al. (2005). Expected changes in water resources availability and water quality with respect to climate change in the Elbe River basin (Germany). *Nordic Hydrology*, 36, 321-333.

Lenderink G., T.A. Buishand & W.P. van Deursen (2007). Estimates of future discharges of the river Rhine using two scenario methodologies: Direct versus delta approach. *Hydrol. Earth Syst. Sci.* 11: 1145-1159.

Liang, X., D.P. Lettenmaier, E.F. Wood & S.J. Burges (1994). A Simple Hydrologically Based Model of Land-Surface Water and Energy Fluxes for General-Circulation Models. *Journal of Geophysical Research-Atmospheres 99*(D7): 14415-14428.

Liu, B.Z., D.Q. Yang, B.S. Ye & S. Berezovskaya (2005). Long-term open-water season stream temperature variations and changes over Lena River Basin in Siberia. *Global and Planetary Change 48:* 96-111.

Lowney, C.L. (2000). Stream temperature variation in regulated rivers: Evidence for a spatial pattern in daily minimum and maximum magnitudes. *Water Resources Research 36:* 2947-2955.

Middelkoop H, K. Daamen, D. Gellens, W. Grabs, J.C.J. Kwadijk, H. Lang, B.W.A.H. Parmet, B. Schädler, J. Schulla & K. Wilke (2001). Climatic change impact on hydrological regimes and water resources management in the Rhine basin. *Climatic Change*, 49: 105-128.

Mohseni, O., H.G. Stefan & T.R. Erickson (1998). A nonlinear regression model for weekly stream temperatures. *Water Resources Research 34:* 2685-2692.

Mohseni, O., T.R. Erickson & H.G. Stefan (1999). Sensitivity of stream temperatures in the United States to air temperatures projected under a global warming scenario. *Water Resources Research 35:* 3723-3733.

Mohseni, O., T.R. Erickson & H.G. Stefan (2002). Upper bounds for stream temperatures in the contiguous United States. *Journal of Environmental Engineering-Asce 128:* 4-11.

Nash, J. E. & J.V. Sutcliffe (1970). River flow forecasting through conceptual models, part 1 - a discussion of principles. *Journal of Hydrology 10:* 282-290.

Nelson, K.C. & M.A. Palmer (2007). Stream temperature surges under urbanization and climate change: Data, models, and responses. *Journal of the American Water Resources Association 43:* 440-452.

Murdoch P.S., J.S. Baron & T.L. Miller (2000). Potential effects of climate chance on surface water quality in North America. *Journal of the American Water Resources Association*, 36, 347-366.

Ozaki, N., T. Fukushima, H. Harasawa, T. Kojiri, K. Kawashima & M. Ono (2003). Statistical analyses on the effects of air temperature fluctuations on river water qualities. *Hydrological Processes 17:* 2837-2853.

Pekarova, P., D. Halmova, P. Miklanek, M. Onderka, J. Pekar & P. Skoda (2008). Is the Water Temperature of the Danube River at Bratislava, Slovakia, Rising? *Journal of Hydrometeorology 9:* 1115-1122.

Piani, C., G.P. Weedon, M. Best, S.M. Gomes, P. Viterbo, S. Hagemann & J. O. Haerter (2010). Statistical bias correction of global simulated daily precipitation and temperature for the application of hydrological models. *Journal of Hydrology 395:* 199-215.

Raskin, P., Gleick, P.H., Kirshen, P., Pontius, R.G. Jr & Strzepek, K. (1997). Comprehensive assessment of the freshwater resources of the world. Stockholm Environmental Institute, Sweden. Document prepared for the 5th session of the United Nations Commission on Sustainable Development.

Rivers-Moore, N.A. & G.P.W. Jewitt (2007). Adaptive management and water temperature variability within a South African river system: What are the management options? *Journal of Environmental Management 82:* 39-50.

Shabalova M.V., W.P.A. van Deursen & T.A. Buishand (2003). Assessing future discharge of the river Rhine using regional climate model integrations and a hydrological model. *Climate Research* 23: 233-246.

Van Den Hurk, B., A. Klein Tank, G. Lenderink, A. Van Ulden, G.J. Ban Oldenborgh, C. Katsman, H. Van den Brink, F. Keller, J. Bessembinder, G. Burgers, G. Komen, W. Hazeleger & S. Drijfhout (2006). KNMI Climate Change Scenarios 2006 for the Netherlands. Royal Netherlands Meteorological Institute, De Bilt,82 pp.

Van der Weijden C.H. & J.J. Middelburg (1989). Hydrogeochemistry of the river Rhine - long-term and seasonal variability, elemental budgets, base levels and pollution. *Water Research* 23: 1247-1266.

Van Vliet, M.T.H. & J.J.G. Zwolsman (2008). Impact of Summer Droughts on the Water Quality of the Meuse River. *Journal of Hydrology* 353: 1-17.

Van Vliet, M.T.H., F. Ludwig, J.J.G. Zwolsman, G.P. Weedon & P. Kabat (2011). Global river temperatures and sensitivity to atmospheric warming and changes in river flow. *Water resources research* 47 (2):W02544.

Webb, B.W. & D.E. Walling (1993). Temporal Variability in the Impact of River Regulation on Thermal Regime and some Biological Implications. *Freshwater Biology 29:* 167-182.

Webb, B.W. (1996). Trends in stream and river temperature. *Hydrological Processes 10:* 205-226.

Webb, B.W. & F. Nobilis (1997). Long-term perspective on the nature of the air-water temperature relationship: A case study. *Hydrological Processes 11:* 137-147.

Webb, B.W., P.D. Clack & D.E. Walling (2003). Water-air temperature relationships in a Devon river system and the role of flow. *Hydrological Processes 17:* 3069-3084.

Webb, B.W. & F. Nobilis (2007). Long-term changes in river temperature and the influence of climatic and hydrological factors. *Hydrological Sciences Journal 52:* 74-85.

Webb, B.W., D.M. Hannah, R.D. Moore, L.E. Brown & F. Nobilis (2008). Recent advances in stream and river temperature research. *Hydrological Processes 22:* 902-918.

Weedon, G.P., S. Gomes, P. Viterbo, H. Österle, J. C. Adam, N. Bellouin, O. Boucher & M. Best (2010). The Watch Forcing Data 1958-2001: A meteorological forcing dataset for land surface and hydrological models. *WATCH Technical report no. 22*, 41 pp.

Weedon, G. P., S. Gomes, P. Viterbo, J. Shuttleworth, E. Blyth, H. Österle, J. C. Adam, N. Bellouin, O. Boucher, and M. Best (submitted), Evidence of changing evaporation in the late twentieth century from the WATCH Forcing Dataset *J. Hydrometeor.*

Zwolsman, J.J.G. & A. Van Bokhoven (2007). Impact of summer droughts on the water quality of the Rhine River - a preview of climate change? *Water Science & Technology* 56: 45–55.

6 Scientific Publications

Peer-reviewed journals

Bonte, M. & J.J.G. Zwolsman (2010). Climate change induced salinisation of artificial lakes in the Netherlands and consequences for drinking water production. *Water Research* 44: 4411-4424.

Van Vliet, M.T.H., F. Ludwig, J.J.G. Zwolsman, G.P. Weedon & P. Kabat (2011). Global river temperatures and the sensitivity to atmospheric warming and changes in river flow. *Water Resources Research* 47, W02544, doi:10.1029/2010WR009198.

Van Vliet, M.T.H. & J.J.G. Zwolsman (2008). Impact of summer droughts on the water quality of the Meuse River. *Journal of Hydrology* 353: 1-17.

Zwolsman, J.J.G. & A. van Bokhoven (2007). Impact of summer droughts on the water quality of the Rhine River - a preview of climate change? *Water Science & Technology* 56 (4): 45–55.

Zwolsman, J.J.G., Johannesen, A., et al. (2009). Climate Change and the Water Industry. *Asian Water*, September 2009: 10-15.

Conference proceedings

Van den Berg, G.A., J. Frijns & J.J.G. Zwolsman, (2009). Implementation of Climate Adaptation and Mitigation Strategies for Drinking Water Production in the Netherlands. In : "Climate Change and Water; International Perspectives on Mitigation and Adaptation" (Editors: Joel Smith, Carol Howe and Jim Henderson), pp. 227-240.

Zwolsman, G, Vanham, D., Fleming, P., Davis, C., Lovell, A., Nolasco, D., Thorne, O., De Sutter, R, Fülöp, B., Staufer, P., Johannessen, Å (2009). Climate change and the water industry – Practical responses and actions. IWA Perspective Document, presented at 5th World Water Forum, Istanbul.

Zwolsman, J.J.G. (2007). Water quality of the Rhine River during summer droughts. Proceedings CHR workshop on low flows and droughts, Würzburg, 25-26 September 2007, p. 109-113.